ECOLE POLYTECHNIQUE FEDERALE DE LAUSANNE
FACULTE DES SCIENCES DE LA VIE

Projet de master en Sciences et Technologies du Vivant

Spatial heterogeneity of functional Magnetic Resonance Imaging indices of dorsolateral prefrontal cortex activation evoked by a working memory task

A comparison of patients with schizophrenia and healthy controls

Réalisé au Athinoula A. Martinos Center for Biomedical Imaging
à Boston, MA, USA
Sous la supervision de Dr. Randy L. Gollub, M.D., Ph.D

Par

Antonia P. Lundquist

Sous la direction de
Prof. Nouchine Hadjikhani, M.D.

Expert externe : Micah Murray, Ph.D.

Lausanne EPFL, 2009

ACKNOWLEDGMENTS

My warmest thank goes to my advisor at the Martinos Center for Biomedical Imaging, Dr Randy Gollub, who gave me insight into the field and much of her time allowing me to evolve in my project.

I thank my supervisor at the EPFL, Dr Nouchine Hadjikhani, for giving me the opportunity to spend this year at the Martinos Center providing me with an unforgettable life experience.

Next, I would like to thank my friends Anastasia Yendiki and Stefan Ehrlich with whom I worked very closely on this project. I thank Stuart Wallace for his availability, technical advices and support and his great help in the finalization of this manuscript. I express my gratitude to Mark Vangel for sharing his deep knowledge in statistics. Furthermore, this project could not have been fulfilled without the technical help of Allison Stevens, Doug Greve, and Nick Schmansky.

Thank you also to my very good friends Lilla Zöllei, Marco Loggia and Chun-yu Yip with whom I have shared many good moments.

Finally, I would like to thank my family for always being there for me.

1 Abstract **1**

2 Abbreviations **2**

3 Introduction **4**

4 Background information **5**

4.1 Schizophrenia: 5
4.1.1 Characteristics 5
4.1.2 Origins of the disease and the dopamine hypothesis 7

4.2 Magnetic Resonance Imaging 8
4.2.1 functional Magnetic Resonance Imaging 8

4.3 Functional localization in the brain 9
4.3.1 Brain anatomy of schizophrenia patients and the lateral frontal lobe 10

4.4 Working memory and schizophrenia 12
4.4.1 Dorsolateral prefrontal cortex and working memory 13
4.4.2 Hypo/hyperfrontality theory 13
4.4.3 Hypothesis on the heterogeneity of DLPFC activation 15
4.4.4 Brain connectivity 16

5 Materials & Methods **18**

5.1 Sternberg Item Recognition Paradigm - SIRP 18
5.2 Subjects 19
5.3 MRI and fMRI 20
5.4 Structural MRI data processing - Freesurfer 21
5.5 Definition of the dorsolateral prefrontal cortex region of interest 21
5.6 Statistical analysis of the fMRI data – FSL 23
5.6.1 First-level analysis 23
5.6.2 Cross-run analysis 26
5.6.3 Group analysis and group comparison 28
5.7 Automation of the analysis - FIPS 28
5.8 Quality assurance - QA 29
5.9 Investigation of the spatial heterogeneity of the activation in the DLPFC 31

6 Results **32**
6.1 Results of the quality assurance 32
6.2 Group mean and group comparison 33
6.3 Study of the fMRI activation indices in the DLPFC 35
7 Discussion **39**
8 Conclusion **43**
9 References **44**
10 Appendix A **51**

1 Abstract

Background: This study is based on the hypothesis that functional Magnetic Resonance Imaging (fMRI) indices in the dorsolateral prefrontal cortex (DLPFC) of schizophrenia patients are spatially more heterogeneous than healthy controls for activation evoked by a working memory (WM) task. Patients have shown to have greater activation than controls in the DLPFC, but this seems to cancel out when performing group averages, which could be explained by patients having more spatially distributed activation. This may one of the causes for discrepant findings concerning hypo- or hyperactivation in the DLPFC of patients when performing a WM task.

Methods: The cohort consisted of demographically matched schizophrenia patients and healthy controls. fMRI data was acquired to study the activation evoked by a modified Sternberg Item Recognition Paradigm (SIRP) known to induce robust activation of the main brain areas subserving WM both in schizophrenia patients and healthy controls. Those areas are the DLPFC, the intraparietal sulcus, the insula and the primary motor cortex. The fMRI data was analyzed with the FMRIB Software Library (FSL). We limited the analysis to the DLPFC by filtering the data with a region of interest (ROI) individually defined for each subject based on its own brain anatomy and conservative Talairach coordinates. For the study of fMRI indices, we used the centers of gravity (COG) of activation clusters. The COG is a 3 dimensional coordinate (x, y, z) computed based on the z-values of all voxels constituting a cluster.

Results: The paradigm induced activation in the brain areas known to be involved in WM. In response to the WM paradigm, the COGs of the activation clusters in the DLPFC had a significantly greater spatial heterogeneity in patients compared to controls in the left hemisphere. The right hemisphere did not show any significant difference between the two groups.

Conclusion: Our hypothesis is supported by our findings in the left hemisphere, but not the right. The methods that were developed for this study are a first attempt to study the spatial heterogeneity of the activation in the DLPFC. The power of the results would benefit from improvement of those methods. In particular, the definition of the DLPFC ROI is to be improved in order to better target the activation patterns of interest.

2 Abbreviations

ART: functional Magnetic Resonance Imaging Artifact Detection Tools
BA: Brodmann area
BET: brain extraction tool
BIRN: Biomedical Informatics Research Network
CT: computed tomography
COG: center of gravity
COPE: contrast of parameter estimate
D_2 receptor: dopamine receptor 2
DLPFC: dorsolateral prefrontal cortex
DSM IV: Diagnostic and Statistical Manual of Mental Disorder, 4th edition
DTI: diffusion tensor imaging
EV: explanatory variable
ED: Euclidian distance
FA: fractional anisotropy
FA: flip angle
fBIRN: Functional Biomedical Informatics Research Network
FE: fixed-effect modeling
FEAT: fMRI Expert Analysis Tool
FILM: FMRIB's Improved Linear Model
FIPS: Functional Biomedical Informatics Research Network (fBIRN) Image Processing Stream
FLIRT: FMRIB's Linear Image Registration Tool
fMRI: functional Magnetic Resonance Imaging
FOV: field of view
FSL: fMRIB Software Library
FWHM: full width at half maximum
GLM: general linear model
IOWA: University of Iowa
IRB: Institutional Review Board
MCFLIRT: Motion Correction using FMRIB's Linear Image Registration Tool
MCIC: Mental Illness and Neuroscience Discovery (MIND) Institute Clinical Imaging Consortium
MGH: Massachusetts General Hospital
MIND: Mental Illness and Neuroscience Discovery
MRI: Magnetic Resonance Imaging
NEX: number of excitations
PE: parameter estimate
PET: positron emission tomography
QA: quality assurance
rCBF: regional cerebral blood flow

RFT: random field theory
ROI: region of interest
SIRP: Sternberg Item Recognition Paradigm
SLF: superior longitudinal fasciculus
SNP: single nucleotide polymorphism
TE: echo time
TR: repetition time
UMN: University of Minnesota
UNM: University of New Mexico
VLPFC: ventrolateral prefrontal cortex
WM: working memory

3 Introduction

Schizophrenia is a psychiatric disease caused partially by genetics and partially by environmental factors. It is currently treated with different kinds of antipsychotic medication. Those treatments have been able to considerably improve patients' daily life, but no drug has yet had the capability to fully cure a patient. Antipsychotic drugs target the dopamine signaling system in the brain thought to be the main cause of schizophrenic symptoms, such as psychosis.

Schizophrenia patients have been shown to be impaired in the performance of working memory (WM) tasks. This impairment underlies many aspects of the disease, such as disorganized speech and difficulties in planning and decision-making based on external stimuli leading to a significant lowering of the quality of life for the affected patients as well as their close surroundings.

In this study we use functional Magnetic Resonance Imaging (fMRI) to investigate whether schizophrenia patients activate the dorsolateral prefrontal cortex (DLPFC), our region of interest (ROI), in a different fashion compared to healthy controls in response to a WM paradigm. We use a modified Sternberg Item Recognition Paradigm (SIRP) in order to elicit activation of the WM network. This hypothesis is based on previous findings suggesting a spatially more heterogeneous activation in patients' DLPFC while performing a working memory task. We use the measure of spatially localized centers of gravity (COG) of clusters of activation in order to assess for the potential differential activation pattern in patients relative to controls.

In the following chapter, we will define the main concepts of this study, which are schizophrenia, functional Magnetic Resonance Imaging, and working memory. In parallel, based on scientific literature, we will present a subset of previous findings that form the foundations for our present hypothesis.

4 Background information

4.1 Schizophrenia:

While schizophrenia is a psychiatric disorder known to alter intelligence, social behavior, affect, it is typically a disorder of cognition (Kandel, Schwartz, & Jessell, 2000). Schizophrenia was at first seen as a purely psychiatric disorder. Nevertheless, with the advancements of neuroscience, it is now clear that schizophrenia has an associated genetic causality (Gur, et al., 2007, p. xxii; Yudofsky & Hales, 1994). Schizophrenia is a neuropsychiatric disease with a worldwide prevalence of about 1%, with a predominance in males (Kandel, et al., 2000). Although schizophrenia has been studied for several decades, there remain many aspects that need to be more thoroughly investigated in order to fully understand the course and outcome of the disease as well as improve its treatment.

4.1.1 Characteristics

Schizophrenia is a heterogeneous syndrome. It is a disease with early onset, usually in late adolescence (Reus, 2008). The Diagnostic and Statistical Manual of Mental Disorders, 4th edition, (DSM IV) (American Psychiatric Association, 1994) describes schizophrenia as the presence of at least two of the five characteristic symptoms listed below for a considerable duration over a one-month time frame:

1. Delusions; 'an idiosyncratic belief or impression that is firmly maintained despite being contradicted by what is generally accepted as reality or rational argument, typically a symptom of mental disorder'[1].

2. Hallucinations; 'an experience involving the apparent perception of something not present'[2].

3. Disorganized speech (e.g. frequent derailment or incoherence).

4. Grossly disorganized or catatonic behavior.

5. Negative symptoms (deficit); i.e. affective flattening, alogia (absurdity, confusion, irrationality, or speechlessness[3]), or avolition (having no will or energy to undertake actions[4]).

[1] ("Oxford American Dictionaries," 2005)
[2] ("Oxford American Dictionaries," 2005)
[3] ("English Wiktionary," 2009)
[4] ("Oxford American Dictionaries," 2005)

Characteristic symptoms 1 to 4 are called psychotic (positive) symptoms in contrast to the deficit (negative) symptoms listed under number 5.

In addition to the characteristic symptoms, an affected person usually has social and/or occupational dysfunction (American Psychiatric Association, 1994). The patient has difficulty in handling the main aspects of daily life, like socializing, handling one's working environment and basic self-care.

DSM IV classifies schizophrenia in five subtypes:

1. *Paranoid type;* the characteristic symptoms are mostly delusions and auditory hallucinations.

2. *Disorganized type;* the prominent symptoms are disorganized speech and behavior, as well as a flattened affect.

3. *Catatonic type;* defined by several features, not all having to be present in one patient: catatonia, excessive and incoherent movements, mutism, and grimacing.

4. *Undifferentiated type;* no symptoms allow a specific classification beyond the characteristic symptoms.

5. *Residual type;* this type is defined as the presence of mostly negative symptoms, and sometimes weakened manifestations of two of the characteristic symptoms.

Patients with schizophrenia are psychosocially impaired and have difficulties in finishing their education. They have impaired neurocognitive functions such as memory, attention, executive functions ('the ability to absorb and interpret information and make decisions based on that information'[5]) and motor speed. This explains some typical facets of the disease like having poor social problem-solving skills, poor community functioning, and not being able to acquire new skills (Green, 1996).

Neuroleptic medications have been proven to treat some psychotic aspects of the disease like hallucinations and delusions, and some atypical antipsychotics have proven successful in improving the WM (Green, et al., 1997). However, most neuroleptics are not successful at significantly ameliorating the cognitive functions needed for a normal daily life (Goldberg & Weinberger, 1996; Ragland, Yoon, Minzenberg, & Carter, 2007). Consequently, more research needs to be done in order to make advancements in the psychosocial and pharmacological treatments of schizophrenia. fMRI studies could lead to a better understanding of what the dysfunctions related to the disease are and to the development of novel therapies aiming at the improvement of patients', as well as their families', quality of life.

[5] ("NIMH: What are the symptoms of schizophrenia," 2009)

4.1.2 Origins of the disease and the dopamine hypothesis

A frequent and mostly unanswered question concerning many psychiatric diseases, including schizophrenia, is what proportion of the causes can be explained by innate (genetics) or acquired (environmental) features. In the case of schizophrenia there are most probably multiple genes involved in disease etiology. In particular, it is very likely that it is caused by the combination of various polymorphisms of the several genes. 6.6% of first-degree relatives of a patient have some form of schizophrenia and the offspring of two schizophrenic people has a 40% risk of developing the disease (Reus, 2008).

Early positron emission tomography (PET) studies have made contradicting observations on the affinity and the density of dopamine receptor (D_2) in the basal ganglia of schizophrenia patients. Some have found a significant increase in D_2 receptors in untreated patients versus controls (Wong, et al., 1986), whereas others did not find any significant difference (Farde, et al., 1990; Martinot, et al., 1990).

Roffman et al. (2008) specify that several genes are involved in causing the disease, and particular combinations of certain genes and polymorphisms could contribute to a higher risk. In particular, the dopamine signaling in the prefrontal cortex is thought to be dysfunctional in schizophrenia patients and impairs their WM. Roffman says the genetics behind it are complex but that the dysfunctioning is partly linked to polymorphisms in the Catechol-O-methyl transferase (COMT) and the methylenetetrahydrofolate reductase (MTHFR) genes. Beyond genetics, the causes of the disease could be a development abnormality, a perinatal injury, or a viral infection (Kandel, et al., 2000).

COMT is considered as a susceptibility gene in the list of various causes of schizophrenia (Reus, 2008). The COMT protein is an enzyme that breaks down the dopamine present in the synapses. Sawaguchi & Goldman-Rakic (1991) have demonstrated the importance of dopamine signaling in the prefrontal cortex of rhesus monkeys for the performance of WM tasks. In the DLPFC in particular, a deficient COMT enzyme leads to partial inhibition of the dopamine inactivation in the synapses. A single nucleotide polymorphism (SNP) in the COMT gene causes a valine amino acid to turn into a methionine amino acid (158Val→Met). People with the methionine allele will have more dopamine in the synapses because of a less efficient COMT enzyme leading to increased dopamine signaling. Drugs reducing dopamine activity (antipsychotic agents) have been successful at treating some symptoms such as psychosis, hallucinations and anxiety, but are often accompanied by several side-effects due to hypoactive dopamine signaling (Reus, 2008). The main principle of action of these drugs is to bind post-synaptically on dopamine receptors D_2/D_3. They are dopamine antagonists.

Related to the DLPFC in particular, dopamine signaling is thought to follow an inverted U-shaped curve, where too much dopamine is as disabling as too little in terms of working memory performance (Roffman, Gollub, et al., 2008).

Also thought to be involved in schizophrenia is a SNP in the MTHFR gene (677C→T) acting indirectly on the dopamine signaling through COMT (Roffman, Gollub, et al., 2008). The MTHFR C/C genotype increases the dopamine in the prefrontal cortex.

But, because of the inverted U shaped curve of DLPFC activation as a function of amount of dopamine, the increase might not always be beneficial. Anyhow, it has been suggested that the T allele on the MTHFR gene in concert with the Val allele of the COMT gene cause significant executive function deficits in schizophrenia patients shifting them to the left of the inverted U performance curve (Roffman, Weiss, et al., 2008).

4.2 Magnetic Resonance Imaging

The advent of brain imaging techniques has revolutionized the way in which brains can be studied. It is namely a noninvasive technique that allows the exploration of multiple features of the brain *in vivo*, anatomically with Magnetic Resonance Imaging (MRI), functionally with fMRI and in terms of connectivity with the more recent technique of Diffusion Tensor Imaging (DTI). The quality and the accuracy of the images resulting from the various MRI techniques are subject to constant evolution and improvements. These techniques present the great advantage, compared to postmortem studies, of allowing the *in vivo* study of diseases such as schizophrenia and thereby link observations made on the functionality and brain structure to actual cognitive deficits and other symptoms.

MR images are acquired with MR scanner. Coils send radiofrequencies exciting the protons (hydrogen atoms), also called spins, in the tissue at their resonance frequency, bringing them to a higher energy state (antiparallel state). When going back to a stable state (parallel state), the nuclei emit electromagnetic energy. The measurement of this energy is what yields the MR signal.

Contrasts between different brain tissues (e.g. white matter, gray matter and cerebrospinal fluid) can be represented in an image due to MRI because it measures the type and the relaxation properties of the atomic nuclei, which are different in different tissues due to the differential molecular composition. This is used for the acquisition of anatomical high-resolution MRI images (T1- and T2-weighted images).

A time constant, T1, defines the time excited high-energy nuclei need to go back the parallel (low-energy) state. The process is called T1 recovery and measures the longitudinal relaxation, i.e. the recovery of the longitudinal magnetization (along the z axis). The T1 contrast is used for acquiring structural MRI scans.

The net magnetization of the spins in the transverse plane (x-y) also decreases over time after the excitation. The spins namely get more and more dephased relative to each other. This is the transverse relaxation process. The time constant defining this process is T2. The contrast is also used for the acquisition of structural MRI scans, but highlight different parameters than the T1 contrast.

4.2.1 functional Magnetic Resonance Imaging

fMRI is the technique used for the study of functional activation of the brain. It is based on the differential electromagnetic properties of oxygenated and deoxygenated

hemoglobin. The proportion of oxygenated relative to deoxygenated hemoglobin in the brain is an indirect measure of the neuronal activity.

For blood-oxygen-level dependent (BOLD)-contrast fMRI, the image acquisition is based on another time constant, the T2*. In addition to the natural dephasing of excited spins measured in T2-weighted images, the external magnetic field causes spatial inhomogeneities in the local magnetic field of the object. The signal decay that is measured is called T2* and is slightly shorter than T2. The applied radiofrequency pulse sequence needs to have a long repetition time (TR, the time interval between two excitation pulses) and a medium long echo time (TE, the time between the excitation pulse and the acquisition of the data). The amount of deoxygenated hemoglobin present in the brain is what describes the intensity of every voxel of the resulting T2*-weighted image. This is possible because oxygenated and deoxygenated hemoglobin react differently to the application of a magnetic field.

Consequently, fMRI indirectly estimates the neuronal activity by measuring the magnitude of the change in deoxygenated hemoglobin present in the vasculature at a certain time. It creates images of the physiological activity, which in turn is correlated with the neuronal activity. T2*-weighted images show a higher signal where the amount of oxygenated hemoglobin is greater (i.e. where neuronal activity is greater). Neural activity requires an increase in local blood flow. The proportion of oxygenated hemoglobin relative to deoxyhemoglobin becomes greater because the supply of oxyhemoglobin exceeds the amount actually needed by the neuronal activity.

Investigating the functionality of patients' brains may help in the long term to link cognitive processes to specific behaviors and symptoms. Also, defining functional patterns and brain morphometry that are unique to schizophrenia patients could ease the diagnosis and serve as points of references for the progression of the disease.

4.3 Functional localization in the brain

Neuroanatomy studies have previously assigned different functions to different locations in the brain based on cytoarchitectonics (Brodmann, 1909). Today, many functions are rather thought to be executed by a particular network of brain areas, and not only requiring a single part of the brain. The consequences of having dysfunctioning areas of the cortex, the white matter, or sub-cortical structures of the human brain can be more or less disabling depending on the cases and the causes. A person with brain damage might show changes in behavior and personality and/or alteration in cognitive processing, such as judgment, memory and intellect.

Before brain imaging, functional localization studies of the human brain were mainly performed on subjects with brain lesions. A detailed examination of their behavior and response to different stimuli could later be partially explained by post-mortem dissections. The development of brain imaging techniques started in the 1970's with computed tomography (CT), and continued with MRI in the beginning of the

1980's[6], and allowed for more rapid, eloquent and concise techniques for functional localization.

4.3.1 Brain anatomy of schizophrenia patients and the lateral frontal lobe

Brain anatomy characteristics of schizophrenia

In (1992), Zigun and Weinberger published results on some particular anatomical observations made on the brains of patients with schizophrenia. Observations that have later been verified by other studies were, as listed in Synopsis of Neuropsychiatry[7]:

Compared to healthy subjects, schizophrenia patients show:

- Enlargement of the lateral ventricles
- Enlargement of the third ventricle
- Dilation of cortical sulci
- Changes in temporal lobe structures

The lateral frontal lobe

The frontal lobe in humans can be separated into several subparts. It is known to be an architectonically very diverse region of the brain (Pandya & Barnes, 1987). Two main subdivisions of the lateral frontal lobe are the dorsolateral part and the frontal operculum.

The frontal operculum includes Brodmann areas (BA) 44, 45 and 47. On the left hemisphere, BA 44 and 45 form Broca's area, which is a key region for the good functioning of language production. A lesion in Broca's area entails aphasia, or the inability to produce speech (Dronkers, Plaisant, Iba-Zizen, & Cabanis, 2007). In the right hemisphere, this area is rather involved in the non-lexical, or paralinguistic, features of language, such as pitch and volume[8].

The dorsolateral frontal lobe of the brain covers BA 8, 9, 46 and 10[9]. In general, lesions in this area in the left hemisphere cause impaired 'verbal intellect', 'defective recency and frequency judgments for verbal material', 'defective verbal fluency' and 'impaired "executive functions"', also called cognitive control, which involves, among other aspects, planning, rule learning, and prevention of inappropriate behaviors[10]. Lesions of the right dorsolateral frontal lobe involve 'impaired nonverbal intellect', 'defective recency and frequency judgments for nonverbal material', 'defective design fluency', as well as impaired "executive functions"'[11].

---

[6] (Tranel, 1994, p. 49)
[7] (Daniel, Zigun, & Weinberger, 1994, p. 146)
[8] (Tranel, 1994, p. 62)
[9] (Tranel, 1994, p. 67)
[10] (Strub & Wise, 1994, p. 199)
[11] (Tranel, 1994, p. 64)

More specifically, the DLPFC is most often defined as covering BA 9 and 46 (Petrides, Alivisatos, Meyer, & Evans, 1993; Rajkowska & Goldman-Rakic, 1995b). Rajkowska & Goldman-Rakic (1995a, 1995b) have described after detailed cytoarchitectonic analyses of several postmortem human brains that BA 9 and 46 are highly variable in terms of location from one brain to another. Yet, beyond those variations, they show that in all individual brains they studied, BA 9 always covered part of the superior frontal gyrus, and BA 46 part of the middle frontal gyrus. They compare their observations with those made by other cartographers (Brodmann, 1909; Sarkissov, Filimonoff, Konokova, Preobrazenskaja, & Kukueva, 1955; von Economo & Koskinas, 1925) and thereby confirmed the intersubject variability. Rajkowska & Goldman-Rakic (1995b) have mapped the area where BA 9 and 46 of the five brains they examined vary and overlap on the Talairach grid system (Fig. 1) (Talairach & Tournoux, 1988) and derived a set of conservative coordinates to describe them. The Talairach atlas is a common reference for using as a standardized space for the study of functional brain imaging. Petrides & Pandya (1999) have further investigated the cytoarchitectonics of BA 9 and 46 and have defined a third area that they call BA 9/46 because it was previously accounted for being part of BA 9 but tends to have similar cytoarchitectonic criteria to BA 46 (Fig. 2). In summary, the frontal lobe is a highly evolved area of the brain and is therefore prone to great interindividual variation (Owen, 2000).

Selemon et al. (2003) made neuronal density studies and found that BA 9 has a significantly higher neuronal density in schizophrenia than healthy controls, whereas other areas of the brain did not show any significant difference, suggesting BA 9 as a target area of the disease.

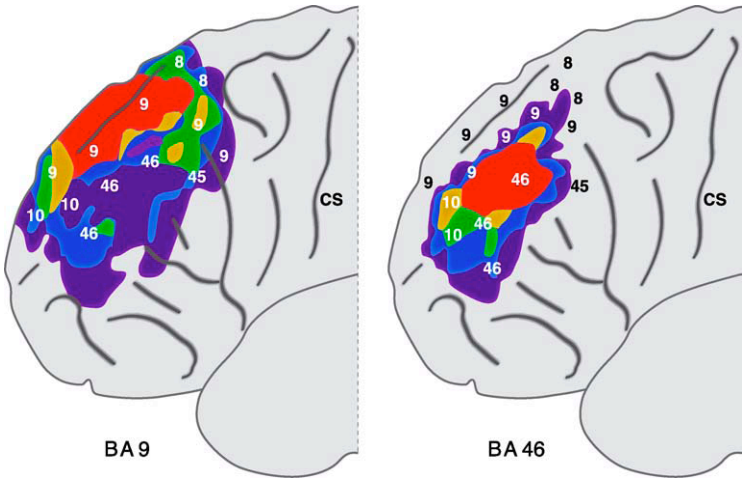

Fig. 1: Cytoarchitectonically defined BA 9 and BA 46 of five brains overlaid on lateral left hemisphere of the Talairach and Tournoux stereotaxic coordinate system. Red shows overlap of the five brains. Dark blue area is covered by only one brain.

(Image taken from (Uylings, Rajkowska, Sanz-Arigita, Amunts, & Zilles, 2005) who adapted it from (Rajkowska & Goldman-Rakic, 1995b))

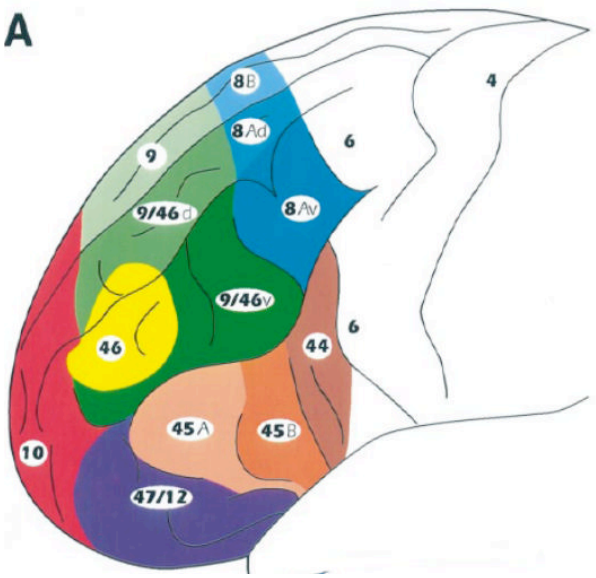

Fig. 2: BA 9, BA 46 and BA 9/46 as defined by Petrides & Pandya (1999).

(Image taken from (Petrides & Pandya, 1999))

4.4 Working memory and schizophrenia

Working memory enables one to simultaneously store and manipulate information temporarily for use in cognitive operations such as understanding language, reasoning and learning, and devising plans for the further guiding of one's behavior (Baddeley, 1992). Baddeley proposed a multicomponent model comprising an attentional control system, the 'central executive', and two underlying systems responsible for temporary storage and manipulation of visual material, the 'visuospatial sketchpad', and verbal material, the 'phonological loop' (Fig. 3). In other words, a functioning WM is critical to successfully remember a phone number during a short time span as well as to perform more demanding cognitive tasks such as behavioral planning.

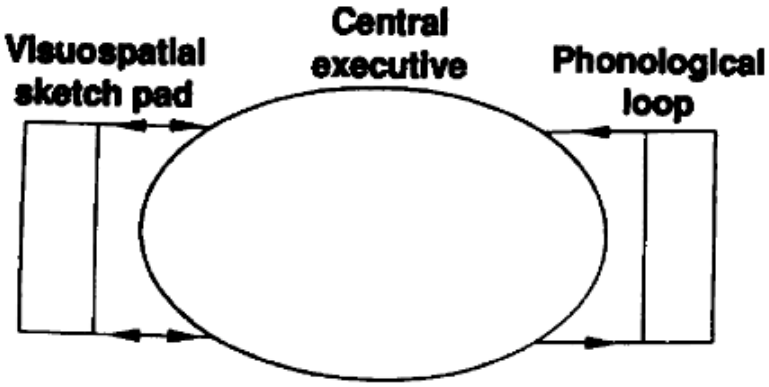

Fig. 3: Baddeley's multicomponent model of working memory.

(Image taken from (Baddeley, 1992))

Consequently, typical signs of schizophrenia, like disorganized speech, thought disorder, avolition or alogia, can be partially explained by an impaired working memory linked to the difficulties in keeping a linguistic plan in mind (Ragland, et al., 2007). Delusions or hallucinations could be the consequences of not having the ability to compare a new stimulus with the associative memories. Several studies have demonstrated that schizophrenia patients show poor skills in the performance of WM tasks (Barch, et al., 2001; Goldman-Rakic, 1994; S. Park & Holzman, 1992).

4.4.1 Dorsolateral prefrontal cortex and working memory

WM tasks are known to involve several brain parts such as the supplementary motor area, the lateral premotor and primary motor areas, the insula, the intraparietal sulcus, and the DLPFC (Cohen, et al., 1997; Jonides, et al., 1998; E. E. Smith, Jonides, Marshuetz, & Koeppe, 1998). This project focuses on the activity in the DLPFC, known to be a key area required for the processing of WM tasks (Goldman-Rakic, 1994; Manoach, et al., 1997; McCarthy, et al., 1996) and robustly responding to the SIRP.

The first studies on blood flow in the DLPFC of schizophrenia patients were performed on subjects in resting state (Ingvar & Franzen, 1974; Petrides, et al., 1993; Weinberger, Berman, & Zec, 1986). This proved to be the wrong approach as there could be no control on the mental activity and hence no reliable replication of results. That is why research groups started to study cognitive aspects instead, giving more insight into task related activation (Ragland, et al., 2007).

Early evidence of the involvement of the DLPFC in the WM network was at first suggested by studies based on humans that had had partial excision of the frontal lobe (Owen, Sahakian, Semple, Polkey, & Robbins, 1995; Petrides & Milner, 1982). Petrides et al. (1993) demonstrated the implication of the DLPFC in the network underlying WM in humans with PET studies. Later, Goldman-Rakic (1994) defined the network involved in working memory in non-human primates. She found with the help of lesion studies, tract tracing, studies of cerebral metabolism and *in vivo* single cell recording that the DLPFC is a key component of the WM network.

4.4.2 Hypo/hyperfrontality theory

Groups have claimed to find both hypoactivation (Berman, Torrey, Daniel, & Weinberger, 1992; Berman, Zec, & Weinberger, 1986; Cannon, et al., 2005; Driesen, et al., 2008) and hyperactivation (Callicott, et al., 2000; Manoach, et al., 1999) of the DLPFC in schizophrenia patients using their WM in fMRI studies. Berman et al. (1986) have demonstrated that both medicated and unmedicated schizophrenia patients have a significantly different regional cerebral blood flow (rCBF) specifically in the DLPFC while performing a WM task and when compared to healthy controls. Healthy controls have an increased blood flow while performing the task, whereas patients don't. The theory claims that the increase in blood flow is correlated to the performance at the task, hence explaining the lower performance of schizophrenia patients. Berman et al. (1992) have also shown a decrease in the rCBF in the prefrontal cortex in schizophrenic twins,

compared to the healthy sibling twin during the performance of a cognitive task, supporting the hypofrontality activation theory of schizophrenia and suggesting it is not caused only by genetics. Driesen et al. (2008) show that the activation in the DLPFC related to a WM task decreases more in patients than controls over time. This hypoactivation in patients does not seem to be linked to medication. Cannon et al. (2005) also claim that schizophrenia patients hypoactivate the DLPFC compared to controls, and prove that this difference is not seen in any other area of the brain involved in working memory task processing.

In contrast, some groups rather claim the hyperactivation of the DLPFC in schizophrenia. The hypothesis behind this is mostly explained by the 'inefficiency' theory: the more difficult the task, the poorer the performance but the more the brain is recruited in order to compensate for the weakened performance. Indeed, patients have shown to activate the DLPFC more than controls but for worse performance at the WM task (Callicott, et al., 2003). More precisely, Manoach et al. (1999) argue for that difference in activation only being significant in the left DLPFC. Manoach et al. (2000) suggest that previous findings of hypoactivation might have been observed because of lack of motivation from the patients' side to perform the task at their best.

Discrepancies between findings of either hypo- or hyperactivation of the DLPFC can be caused by different tasks used in different studies, making the studies incomparable. Even if all tasks require the use of WM, some widely used ones, like the Wisconsin Card Sorting Test, also tests for other functions (e.g. task switching, maintenance of attention, concept formation (Sullivan, et al., 1993)).

The relation between activation in the DLPFC and increasing WM load is not a linear one. It has been observed that both for patients (Manoach, 2003) and healthy controls (Callicott, et al., 1999; Goldberg, et al., 1998) activation in the DLPFC may decrease or simply not increase anymore when reaching a certain level of cognitive load, i.e. a level that exceeds the subject's capacity. That is, when the task becomes too complex, the activity in the DLPFC is not increasing anymore, or even decreases, while performance declines. That cognitive load threshold at which performance starts to decline is lower for patients than for controls. This model corresponds to an inverted U-shaped curve of DLPFC activation versus increase in working memory load (Fig. 4). The hypoactivity found in some studies might be caused by tasks using too high loads of working memory. When the complexity of a task exceeds a manageable threshold, subjects may start guessing or simply feeling helpless and not focus on the assignment anymore (Manoach, 2003).

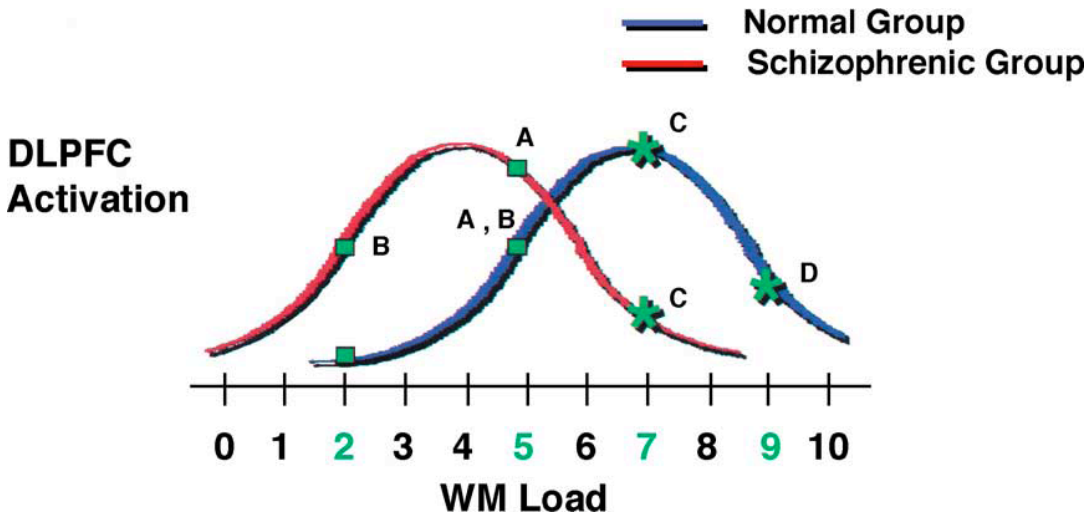

Fig. 4: Increase in working memory load shows an inverted-U shaped curve of the activation in the DLPFC. The maximum activation is attained at lower memory loads for schizophrenia patients compared to healthy controls.

(Image taken from (Manoach, 2003))

Karlsgodt et al. (2009) have come up with a new model to explain these differences in activation. They further separate groups of patients and controls into high and low performers. They claim and demonstrate that high performing controls need fewer resources to complete the same task as low performers, causing low performing controls to hyperactivate, leading to a greater percent signal change from baseline. In contrast, high performing schizophrenia patients seem to activate the DLPFC significantly more that low performing ones.

4.4.3 Hypothesis on the heterogeneity of DLPFC activation

Manoach et al. (2000) found a novel way of explaining the hypofrontality found by certain groups. First, they suggest that the impaired working memory in schizophrenia may be caused either by dysfunction of the DLPFC or some remote cortical or subcortical structure regulating the DLPFC. Moreover, they show that the fMRI indices of activity in the DLPFC of patients are not overlapping those of the controls. Most of the areas that both patients and controls activate in common show notable overlap, except for the DLPFC. They analyzed results from both individual subjects and averaged group data. Interestingly, they found that in individual subjects, schizophrenia patients had a larger number of active voxels in the DLPFC than controls. However, when subjects were averaged together into groups of patients versus controls, the number of active voxels in the DLPFC was larger for healthy controls. The following observation was that only 24% of the activation clusters in each patient overlapped the patient's group cluster, whereas the controls showed a 71% overlap with the control's group cluster. Relative to controls, schizophrenic subjects are therefore thought to have higher but more spatially heterogeneous activation in the DLPFC. Hypoactivation in the frontal

lobe of patients performing WM tasks has nevertheless been shown in individual subjects (Barch, et al., 2001; Stevens, Goldman-Rakic, Gore, Fulbright, & Wexler, 1998). Weinberger & Berman (1996) and Holt et al. (1999) have confirmed the aberrant activation of the DLPFC in schizophrenia patients related to WM tasks compared to healthy controls.

Another interesting hypothesis is that schizophrenia prevents the automation of a task thereby leading to more variability in the results after several repetitions compared to healthy controls. A normal subject would learn the best way of treating a task and adapt with time. But a patient repeating a task would have a hard time building up a strategy. Automation results in greater efficiency and more behavior and spatially more reliable patterns of activation (Manoach, 2003).

4.4.4 Brain connectivity

Cohen et al. (1997) have suggested the involvement of both frontal and parietal brain areas in the processing of WM tasks. Petrides (1996) even discriminated the connection from the parietal cortex to the ventrolateral prefrontal cortex (VLPFC) and the DLPFC depending on the type of processing. The functional connection between the VLPFC and the DLPFC has been shown to be very strong (R. Schlosser, et al., 1998). Schlosser et al. (2003) have later suggested that medicated schizophrenia patients show a reduction of the prefrontal-cerebellar connectivity, but a strengthened thalamo-cortical connectivity. DTI studies have suggested changes in the structure of the white matter in the medial temporal lobe and the DLPFC of the right hemisphere of schizophrenia patients, and a correlation between the hemodynamic response of the DLPFC and this reduction in white matter (R. G. Schlosser, et al., 2007).

The main white matter connection between the frontal and the parietal cortex is the superior longitudinal fasciculus (SLF). DTI measures the fractional anisotropy (FA), which is correlated to the integrity of the white matter. Karlsgodt et al. (2008) have found a reduction in the FA of the SLF in schizophrenia patients, especially in the left hemisphere. Interestingly, they could link that reduction of the FA to a lower performance at a verbal WM task emphasizing the functional importance of the fronto-parietal connectivity. Hence, abnormalities in the white matter of patients may cause differential patterns of activation as compared to healthy controls.

Makris et al. (2005) use *in vivo* DTI to show that the SLF can be divided into four subcomponents as previously found in non-human primates (Petrides & Pandya, 1984). They suggest that the findings made in primates can be translated to humans and report that the SLF is in fact four separate fascicles: SLF I, SLF II, SLF III, and the arcuate fascicle (AF), all lying adjacent to one other.

SLF I was found to connect the medial/dorsal parietal lobe to both dorso-frontal/dorso-medial prefrontal regions and dorsal premotor areas. SLF II, said to be the main subdivision of the SLF, was shown to run from the angular gyrus (caudal-inferior parietal area) to the caudal-lateral prefrontal area/middle frontal gyrus (BA 6, 8 and 46) passing on top of the insula. SLF III was suggested to connect the supramarginal gyrus to

the ventral premotor and prefrontal areas. The arcuate fasciculus runs from the posterior part of the superior temporal gyrus to the lateral prefrontal cortex (BA 8 and 46), passing over the insula and the Sylvian fissure, joining the SLF II. Makris et al. suggest the function of SLF II to be involved in the understanding of the visual space. The group also suggests the possibility that SLF II has a role in spatial working memory, because of its connection to BA 46.

5 Materials & Methods

5.1 Sternberg Item Recognition Paradigm - SIRP

A modified version of the SIRP was used to assess WM (Sternberg, 1966). The SIRP is a block design task consisting of a phase of encoding of a set of 1, 3 or 5 digits (load 1 = low, load 3 = medium or load 5 = high WM load) followed by a blocked sequence of 1-digit probes (Fig. 5). This paradigm has been previously shown to consistently activate the DLPFC in healthy controls and schizophrenia patients, both performing above chance level (Manoach, et al., 1999; Manoach, et al., 1997; Rypma, Prabhakaran, Desmond, Glover, & Gabrieli, 1999).

The subject had to report whether the probe digit was part of the encoding sequence (a target) or not (a foil). Subjects responded by pressing the 'target' or the 'foil' button, the buttons were randomly assigned to either the right or the left thumb (one button in each hand) according to their study ID to prevent handedness effects. Subjects were directed to be as accurate and quick as possible. There was a $0.05 bonus for every correct response to prevent lack of motivation and biased results.

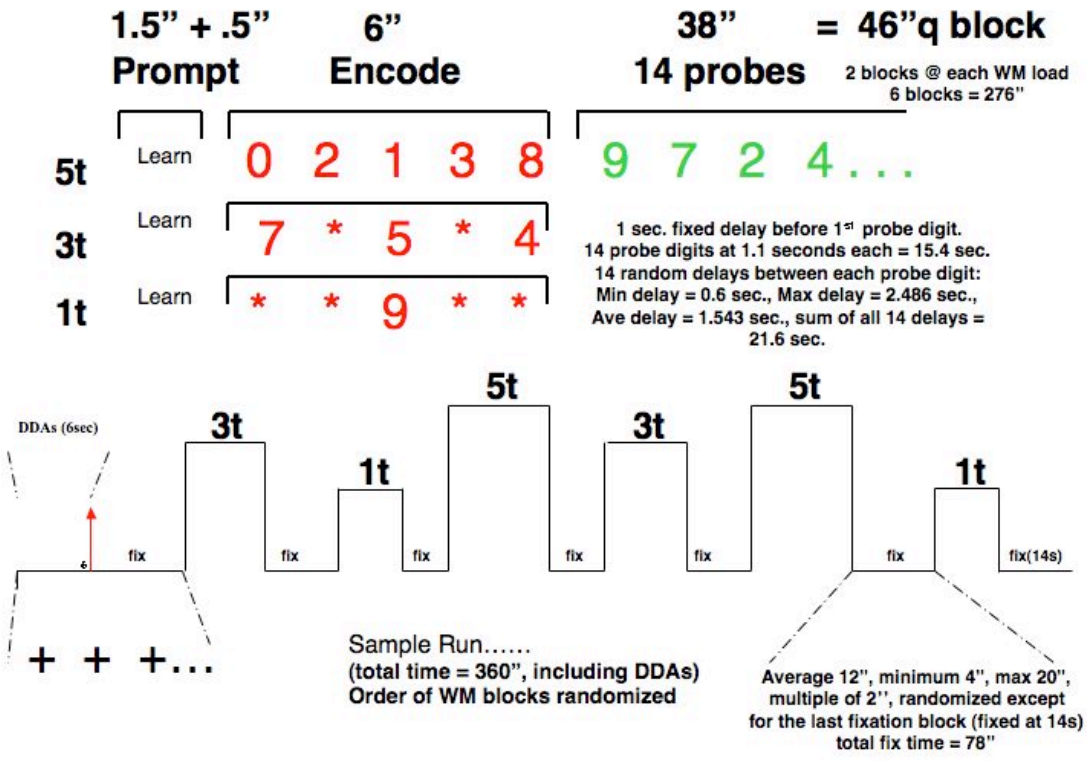

Fig. 5: The Sternberg Item Recognition Paradigm. See text for details.

The subjects underwent three runs of the task in total. Each run comprised 2 blocks of each memory load presented in a random order, for a total of 6 blocks per run. A run started with 6 seconds of fixation on a cross. The subject was then prompted for 1.5 seconds by the word 'Learn' displayed on the screen (*learn* condition). After a 0.5 second delay, a sequence of 1, 3 or 5 digits, depending on the task's load, appeared for 6 seconds in red (*encode* condition). Following a 1 second delay, the 14 probes were displayed one after the other in a random sequence for 1.1 seconds each in green with a random delay of 1.543 seconds on average between every probe (*probe* condition). Half the probes were targets, and half were foils. The duration of a block was 46 seconds with a random fixation time between every block being 12 seconds on average, and the last fixation block being set to 14 seconds. Therefore, a run totaled 360 seconds in duration. The paradigm was programmed with the EPrime presentation software, which also recorded the behavioral response information (reaction time and accuracy).

5.2 Subjects

All brain imaging data had been originally collected as part of the Mental Illness and Neuroscience Discovery (MIND) Institute Clinical Imaging Consortium (MCIC) Study. This consortium was created for the study of first-episode and chronic schizophrenia. Its primary clinical aim is the identification of the neural substrates of the core cognitive deficits associated with schizophrenia, their link to the clinical features of the disorder and their alterations with disease progression and treatment. It is a partnership between four sites: the University of New Mexico (UNM), the University of Minnesota (UMN), the University of Iowa (IOWA) and the Massachusetts General Hospital (MGH).

The following study is limited to the subjects coming from the MGH site. Initially there were 64 subjects: 38 patients and 26 matched controls. 59 subjects (35 patients and 24 controls) passed the quality assurance for the whole brain analysis. 47 subjects passed the quality assurance process for the ROI analysis (see section 5.8), whereof 32 were patients and 15 were controls. The controls were demographically matched to the patients with regard to gender, age, education and parental socioeconomic status (Table 1). Schizophrenia diagnosis was based on the criteria listed in the DSM IV, and a Structured Clinical Interview for DSM disorders (SCID).

Table 1: Demographic data. Means, standard deviations and group comparisons.

Subject characteristics	Normal subjects (n=15)	Schizophrenic subjects (n=32)	t	p
Gender (% female)	33	28	-	-
Age	40.67 ± 9.74	37.34 ± 10.15	0.3	0.38
Education (years)	15.68 ± 2.01	12.03 ± 2.69	2.34	0.99
Parental socioeconomic status (low score denotes high status)	2.93 ± 0.77	3.2 ± 1.02	0.31	0.76

5.3 MRI and fMRI

Structural Magnetic Resonance Imaging – MRI:

Both T1 (MP-RAGE) and T2 gradient-echo (GRE) anatomical scans, as well as phase and magnitude field maps for image distortion correction, were acquired on a 1.5 Tesla Siemens Sonata scanner. The scanning parameters are listed in Table 2.

Table 2: MRI scanning parameters. T1 scan: acquired with a spoiled GRASS (gradient recalled acquisition in the steady-state) sequence. T2 scan: echo train length of 1.

Parameters	Repetition time (TR) (msec)	Echo time (TE) (msec)	Flip angle (FA) (°)	Field of view (FOV) (cm)	Matrix	Number of excitations (NEX)	Acquisition time (min)	Slice thickness, coronal slices (mm)
T1 scan	12	5	20	16x16	256x256	3	~22	1.5
T2 scan	9000	64	2	16x16	256x256	2	~18	

Functional Magnetic Resonance Imaging - fMRI:

All functional brain imaging was performed with a 3-axis gradient head-coil in a 3 Tesla Siemens Trio system equipped for echo planar imaging. Phase and magnitude field maps were acquired to correct for image distortion (scan time: 1.5 min).

The SIRP requires 180 time points for a scan length of 6:00 minutes. The three first scans were discarded (3 DDAs) allowing the longitudinal magnetization to stabilize. The scanning parameters are listed in Table 3.

Table 3: fMRI scanning parameters. Images were acquired using a gradient echo T2*-weighted sequence with an in-plane resolution of 3.1 mm.

Parameters	TR (msec)	TE (msec)	FA (°)	Band-width (BW) (kHz)	FOV (cm)	Matrix	Number of slices	Slice thickness (mm)	Slice orientation
T2* scan	2000	30	90	>+/- 100	22	64x64	27	4, with 1 gap	AC-PC line

5.4 Structural MRI data processing - Freesurfer

All the subjects' structural MRI data had been previously processed. Cortical reconstruction and volumetric segmentation based on high resolution structural MRI scans was performed with the Freesurfer surface reconstruction software (Fischl, et al., 2002), which is documented and freely available for download online[12].

Freesurfer automatically identifies different structures of the brain and classifies all the brain tissue into gray matter, white matter or cerebrospinal fluid (CSF). It generates white matter and pial brain surfaces and assigns a neuroanatomical label to every voxel of the MRI volume (37 different labels in total). Further, it estimates the brain's volume and cortical thickness. After processing and surface rendering, every subject's brain has a cortical parcellation map and a subcortical segmentation map. Options to visualize the brain's surface in 3 dimensions are also available either as pial/white matter surface, or inflated (gray/white matter interface), or even flattened depending on one's needs. Parcellation maps can be overlaid on the brain's surface. The subcortical segmentation can also be viewed overlaid on the structural image. Further, low-resolution functional data can be overlaid on the reconstructed brain, after applying the appropriate registration, for easy localization of brain activation.

5.5 Definition of the dorsolateral prefrontal cortex region of interest

As described in the introduction (see 4.3.1), the localization of the DLPFC in the human brain is considerably variable. Most often, the DLPFC is described as covering BA 46 and the lateral part of BA 9. From this description we created a ROI label for the DLPFC derived from the Freesurfer cortical parcellation map (Fischl, et al., 2002) and the use of conservative Talairach coordinates based on cytoarchitectonic studies (Fig. 6) (Rajkowska & Goldman-Rakic, 1995b) (Area 9: anterior/posterior (AP) +53 to +26, dorso/ventral (DV) +50 to +25; Area 46: AP +50 to +29, DV +36 to +14). The superior frontal gyrus, the rostral middle frontal gyrus and the caudal middle frontal gyrus Freesurfer parcellations were merged to form a dorsal prefrontal label. A coronal cut was applied on the latter ROI at Talairach coordinate y = 26 to conform it to the conservative Talairach criteria described in Rajkowska & Goldman-Rakic (1995b). A subsequent cut was made to separate the medial part from the lateral one on the superior edge of the medial wall of the brain (Fig. 7). This way, the ROI was individually defined for every subject to optimize subject specificity. The anatomically defined DLPFC ROI was then registered to the functional scans of every individual subject for further use in the fMRI analysis.

Because of the previously mentioned inter-subject variability in the localization of the DLPFC, the definition of the boundaries of the DLPFC varies between studies. Potkin et al. (2009) use the WFU Pickatlas in MNI space (Maldjian, Laurienti, & Burdette, 2004; Maldjian, Laurienti, Kraft, & Burdette, 2003), while Wisco et al. (2007) limit their DLPFC

[12] http://surfer.nmr.mgh.harvard.edu/ ("Freesurfer surface reconstruction software,")

to a part of the Freesurfer rostral middle-frontal label. Our definition of the DLPFC is still to be improved based on future findings.

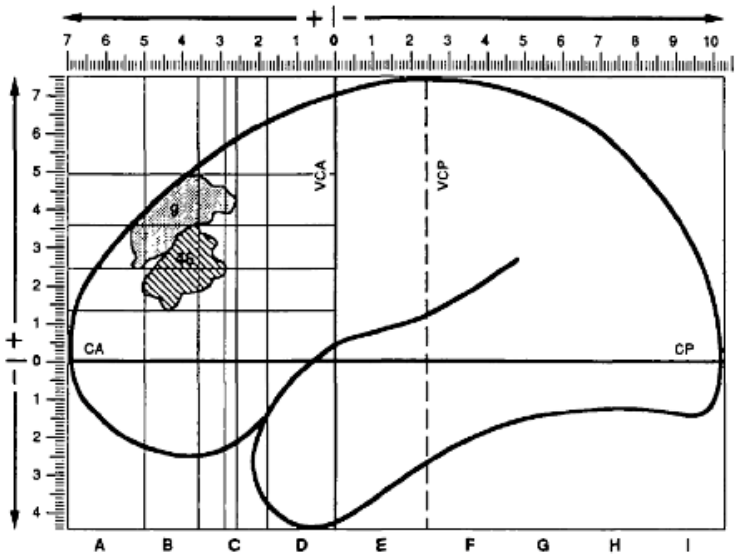

Fig. 6: Left hemisphere of the Talairach and Tournoux grid system displaying the conservative Talairach coordinates of BA 9 and BA 46 as defined by Rajkowska and Goldman-Rakic (1995b).

(Image taken from (Rajkowska & Goldman-Rakic, 1995b))

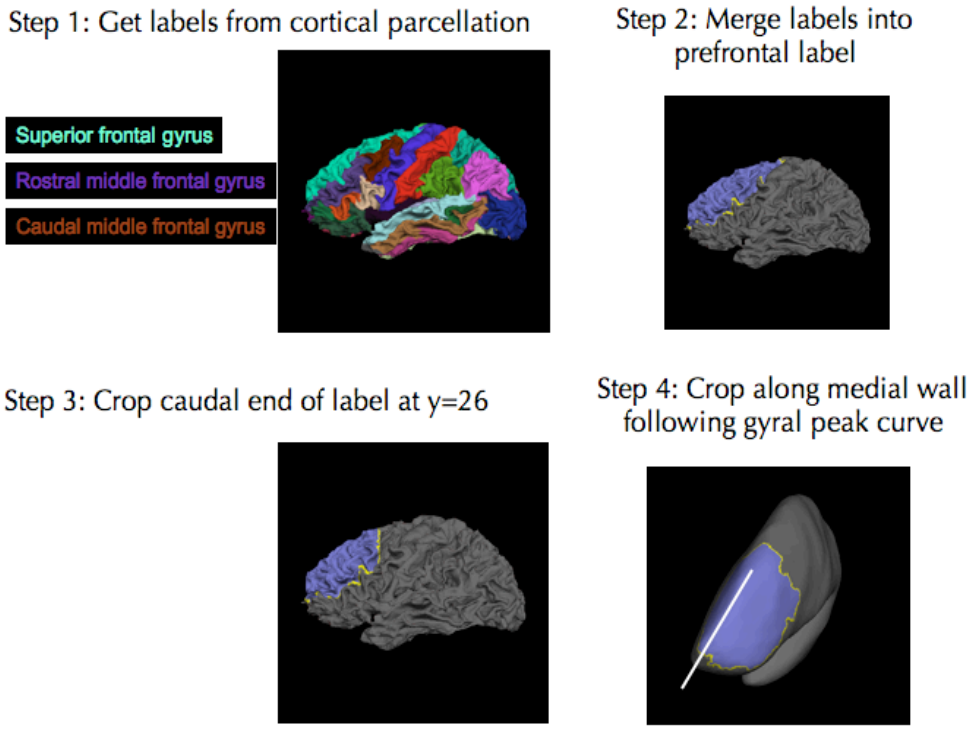

Fig. 7: The fours steps required for the creation of the DLPFC ROI.

5.6 Statistical analysis of the fMRI data – FSL

The Functional Magnetic Resonance Imaging of the Brain (fMRIB) Software Library[13] (FSL) was developed by the fMRIB analysis group in Oxford, UK. This software package is comprised of tools for the analysis of MRI, fMRI as well as DTI data from simple preprocessing steps such as non-brain voxel removal (the brain extraction tool - BET) to the elaborate fMRI Expert Analysis Tool (FEAT). FEAT is a very complete tool, in which one can set different parameters, like motion correction, intensity normalization, and registration to either a standard brain or a high-resolution image of a particular subject's brain. Statistical analysis in FEAT is based on univariate general linear modeling (GLM), also known as multiple regression modeling. Univariate, as opposed to multivariate, means that the model is applied to a single voxel at a time and not to the whole volume.

One can perform first level analysis of single runs of fMRI data, as well as average across several runs from one subject (cross-run analysis). Completion of a second-level FEAT analysis groups and averages cross-run analysis from several subjects. Finally, in the third-level analysis, one can compare different groups' results, e.g. patients versus controls. Analysis was carried out using FEAT Version 5.92.

5.6.1 First-level analysis

pre-statistics

The following processing was applied:

1. Motion correction corrects for the movement of the subject's head in the scanner. It uses the FMRIB's Linear Image Registration Tool (MCFLIRT) (Jenkinson, Bannister, Brady, & Smith, 2002). Motion correction estimates the motion from one time frame to the next (relative motion), but also from each time point to a reference image, the middle time frame (absolute motion). It uses rigid-body transformation. That means 6 degrees of freedom: 3 translations and 3 rotations (roll, pitch and yaw) along the three axes x, y and z.
2. Non-brain removal using the brain extraction tool (BET) (S. M. Smith, 2002). This removes all skull and non-brain tissue and allows for unwanted voxels to not be taken into account in the fMRI analysis.
3. Spatial smoothing using a Gaussian kernel of full width at half maximum (FWHM) of 5 mm. The aim of spatial smoothing is to increase the dependency between one voxel and its neighbors, and to reduce noise without canceling out significant activation. It

[13] http://www.fmrib.ox.ac.uk/fsl ("FSL - FMRIB Software Library,")

assumes that the signal is more spatially correlated than the noise, which improves the signal-to-noise ratio.
fMRI data is namely already spatially correlated before smoothing because two voxels lying next to each other have a high probability of representing two points in the brain having the same function. Additionally, the vascular system introduces blurring in the measured signal further increasing the inherent spatial correlation of fMRI data.
Spatial smoothing also permits the use of the Random Field Theory (RFT) instead of the Bonferroni correction in order to correct for multiple comparisons induced by the GLM. The problem of multiple comparisons is that the probability of finding false positives (Type I error) is linearly correlated with the number of statistical tests. Bonferroni correction is too conservative for spatially correlated data and increases Type II errors (false negatives, i.e. missing true activation). The RFT reduces the value of the number of independent statistical tests based on the smoothness of the data[14].

4. Highpass temporal filtering to remove low frequency artifacts.

Statistical analysis:

Time-series statistical analysis was carried out using FMRIB's Improved Linear Model (FILM). In the GLM, a model that represents the signal expected to be found in the data is created based on the experimental design. For the SIRP block design, there are 7 explanatory variables (EV's) (see the design matrix in Fig. 8): one for the time when the word 'learn' is displayed on the screen (lrn), one for the encoding period of all three loads (e1, e3, and e5), and one for the probing session of each load (p1, p3 and p5). The timing of these EV's is extracted from the stimulus schedule of the SIRP. The waveform of the EV's is then convolved with a hemodynamic response function (a gamma function with a half-width of 3 standard deviations and a mean lag of 6 seconds) in order to best fit the timing of the activation in the brain that slightly lags the actual stimulus because of physiological reasons.

[14] (Huettel, Song, & McCarthy, 2004)

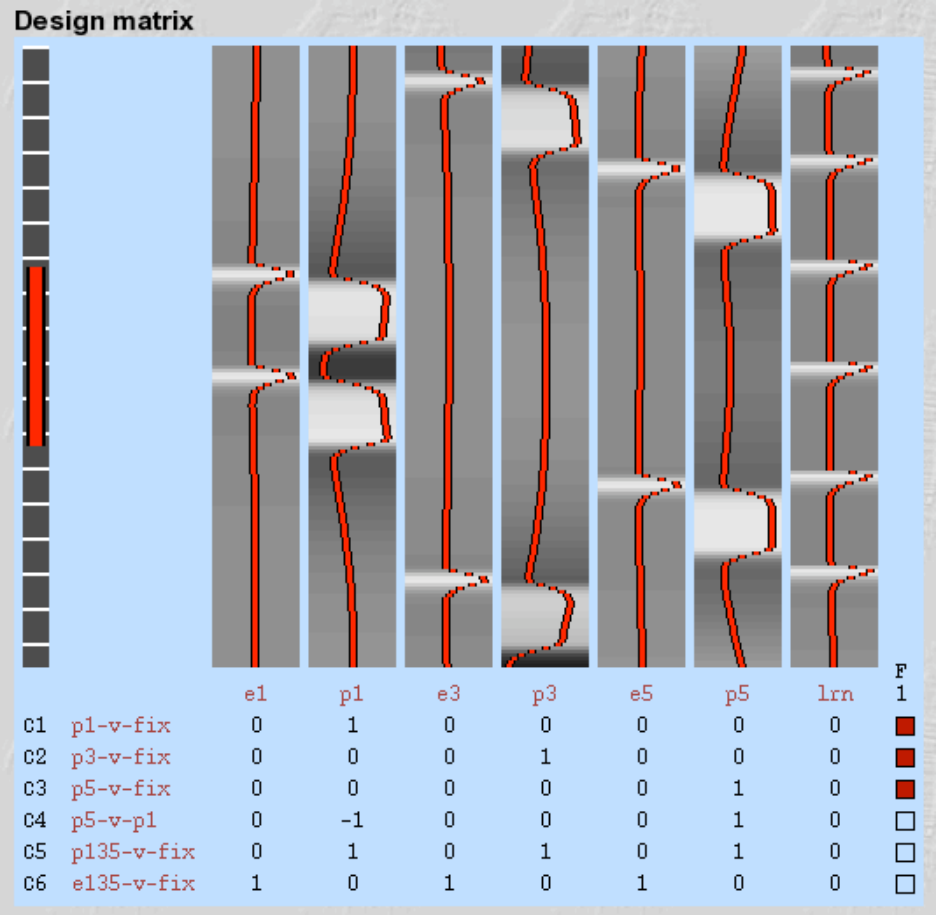

Fig. 8: Design matrix for lower-level analysis. See text for details.

Parameter estimates (PE's) of every EV are then generated for every voxel depending on how well that voxel's time-course fits the model. PE's are then converted into statistical maps. In the model, one can also compare PE's by setting up contrasts of PE's (COPE) as well as F-tests to test for the association to the data of one EV related to another or to the baseline. A statistical image is created for every COPE. Our model has six COPES and one F-test:

1. p1-v-fix: load 1 versus baseline. The Z statistic output image will display the activation produced by the probing sequences of load 1.

2. p3-v-fix: load 3 versus baseline. The Z statistic output image will display the activation produced by the probing sequences of load 3.

3. p5-v-fix: load 5 versus baseline. The Z statistic output image will display the activation produced by the probing sequences of load 5.

4. p5-v-p1: load 5 versus load 1. This compares two stimulus types by subtracting one EV to another. Activation produced by both probe 1

and probe 5 is canceled by the subtraction. The resulting statistical map shows brain areas active for load 5 only, i.e. shows the load specific activation.

5. p135-v-fix: sum of probe 1, probe 3 and probe 5. The statistical output is a sum of the activation resulting from each load during the probe epoch. Equal weight is given to all loads (e.g. is load independent). It is statistically useful to identify voxels that are more active during the overall task and within which to hunt for load specific activation.

6. e135-v-fix: sum of encoding 1, encoding 3 and encoding 5. The statistical output is a sum of the activation resulting from each load during encoding.

- F-test between probe 1, probe 3 and probe 5. The statistical output of the F test displays the regions of the brain in which there is activation for either loads. That is, it shows whether there is a general effect of probing task versus baseline.

Registration:

Registration of low resolution functional images to high resolution standard space images (MNI 152[15]) was carried out using FMRIB's Linear Image Registration Tool (FLIRT) with 12 degrees of freedom, allowing scaling and shearing of the image in addition to translation and rotation (Jenkinson, et al., 2002; Jenkinson & Smith, 2001). Registration to standard space is necessary in order to further analyze the data, averaging across the runs and performing group analysis.

5.6.2 Cross-run analysis

The cross-run analysis is based on fixed-effect (FE) modeling. It consists of a simple average across all three runs for each subject (see design matrix in Fig. 9), and increases the signal-to-noise ratio assuming that the signal is the same in all runs, while the noise is random. It tells us where the subject activates on average for each of the previously specified COPEs. FSL takes as input the three first-level analysis output files.

[15] Montreal Neurological Institute average of 152 brains of normal subjects. www.mni.mcgill.ca ("Montreal Neurological Institute,")

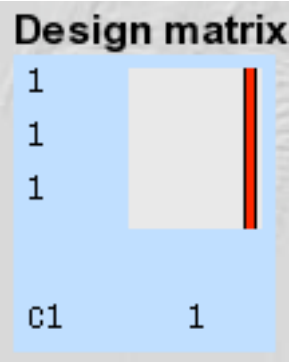

Fig. 9: Design matrix for the cross-run analysis.

Post-statistics:

One can constrain the analysis to a specific area or ROI by applying a mask on the functional data before the completion of analysis. We performed pre-threshold masking with the DLPFC ROI labels in order to restrict the extraction of clusters.

The original Z-statistic images were thresholded using $z>2.3$, and clusters were then tested for significance using RFT with a final significance test of $p = 0.05$ corrected for multiple comparisons (Forman, et al., 1995; Friston, Worsley, Frakowiak, Mazziotta, & Evans, 1994; Worsley, Evans, Marrett, & Neelin, 1992). The threshold for the minimum size of a cluster is based on the number of voxels in the whole dataset. FSL outputs a volume with every cluster being assigned a different color for easy visualization. The clusters are also reported in a numerically indexed list containing the following data:

- A cluster index from 1 to n, n being the biggest cluster found in the volume
- The number of voxels in each cluster
- The p-value of the cluster
- The z-value of the maximally active voxel of the cluster, as well as up to six other local maxima included in the same cluster
- The coordinates of the maximally active voxel, and local maxima found within each cluster
- The center of gravity (COG) of the cluster computed based on a weighting of the z-value of all voxels comprised in a cluster
- The coordinates of the voxel with the maximum percent signal change from baseline for the COPE of interest

- The percent signal change of that voxel
- The mean percent signal change across all voxels included in the cluster

5.6.3 Group analysis and group comparison

We performed a whole brain group analysis for both patients and controls using mixed effects analysis that allows extrapolating the results to the general population that the subjects were drawn from. We also performed group comparisons in order to determine whether patients have a different activation pattern relative to controls (two-sample unpaired t-test) (see design matrix in Fig. 10). The group means and the group comparisons were only performed on contrast 5, that sums the activation induced by all three loads of the paradigm.

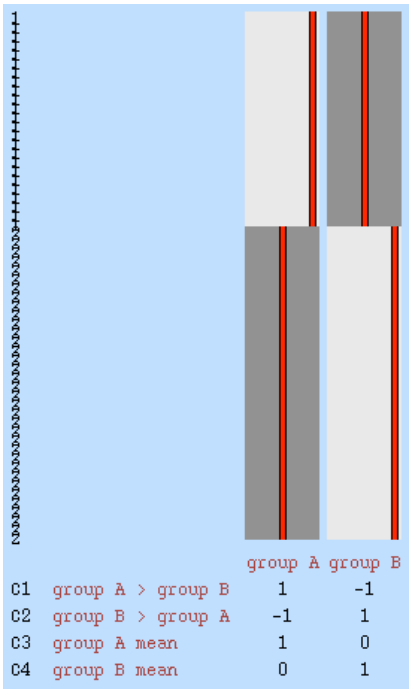

Fig. 10: Design matrix for the group comparisons and the group means. Group A: controls. Group B: patients. (59 subjects: 35 patients and 24 controls)

5.7 Automation of the analysis - FIPS

The Functional Biomedical Informatics Research Network (fBIRN) Image Processing Stream (FIPS)[16] was also used for data analysis. Originally created for data acquired by the Biomedical Informatics Research Network (BIRN[17]) under the direction

[16] https://xwiki.nbirn.net/xwiki/bin/view/Project-FIPS-Public/Home ("FIPS Wiki,")

[17] a consortium developing methods for multi-site functional imaging studies. http://www.nbirn.net/ ("Biomedical Informatics Research Network (BIRN),")

of the National Institute of Health (NIH), necessary changes to its processing stream were made to be compatible with the MCIC data. FIPS is a software package that allows for the automated management of large multi-site fMRI studies. It provides a very specific data hierarchy for making its usage accessible to anyone with large neuroimaging datasets while simplifying the sharing of information. FIPS uses both FSL and Freesurfer as computational engines. The majority of the FSL functional image analysis was automated with FIPS. FIPS can also be used for easy visualization of the statistical analysis through Freesurfer. The output of the functional data is namely registered to the anatomical data preprocessed with Freesurfer.

5.8 Quality assurance - QA

The quality assurance (QA) of the data is a key step for the successful outcome of the analysis. There are different reasons that can cause a subject's data to be classified as being of too poor quality to be processed without compromising the power of the analysis. The QA processing for this data was the following:

Disenrolled subjects:

According to the rules of the Institutional Review Board (IRB), any subject had the right to disenroll from the study at any time without further explanation. That data is not to be used for any analysis.

Behavioral criteria:

Missing data was defined as a block completed with less than a 70% accuracy rate (10 out of 14 correctly identified), and/or with more than 6 probes not answered within a block. Subjects that missed four or more of the 18 SIRP blocks comprising the task (three runs, with six blocks per run) were considered as behavioral dropouts. They were not further processed into the analysis.

Missing behavioral data not due to subject error:

Technical issues can cause behavioral data (reaction time and accuracy) to not be recorded as subjects are performing the task. The functional data is nevertheless acquired normally. Those cases were retained for the functional analysis.

Freesurfer processing of the structural data:

The quality assurance of the Freesurfer processing of the structural data was semi-automated with a tool embedded in the Freesurfer software package. The tool checked whether any step of the processing was missed, and captured snapshots of the following:

- The subcortical segmentation: 7 coronal slices and one sagittal slice per hemisphere of the skull-stripped brain.
- The white and pial surfaces: 7 coronal slices and one sagittal slice per hemisphere of the skull-stripped brain.

- The inflated brain: a lateral, a medial, and an inferior view of both the right and the left inflated hemispheres.
- The curvature map: a lateral, a medial and an inferior view of the curvature map (gyri in green, and sulci in red) overlaid on both hemispheres of the inflated brain.
- The cortical parcellation: a lateral, a medial and an inferior view of the cortical parcellation overlaid on both hemispheres.

We later examined those snapshots for every subject searching for abnormalities in the skull stripping and/or in the white and pial surface delineation. If an abnormality was found, we performed minimal edits according to the Freesurfer standard manual before rerunning the Freesurfer processing on the problematic subjects.

Registration to high-resolution anatomical image:

We used a Freesurfer tool for a boundary-based registration of the functional data to the high-resolution structural data. We manually checked a subset of the subject's registrations.

Brainmask:

The brainmask is a binary volume created by FSL based on the first functional MRI volume after brain extraction. It is meant to cover all voxels belonging to the brain only, but the algorithm does not always successfully classify every single voxel as brain or non-brain. Also, bad positioning in the scanner can cause the functional scans to not cover the whole brain. The resulting brain-mask can therefore be of somewhat insufficient quality. This may cause problems at the level of group analysis as the masks from all subjects are concatenated to create a group mask. The group mask only includes voxels where every single subject presents a voxel in its individual mask. Masks were checked manually at the cross-run level, and, if corrupted, further checked at the first level for missing slices due to bad positioning of the subject in the scanner. Subjects with badly corrupted masks were discarded from the analysis.

Motion and mean intensity of functional data:

We used the fMRI Artifact Detection Tools (ART) developed by Whitfield-Gabrieli (2009) to perform automated detection of outliers, both for motion and global mean image intensity. The program was set to flag time frames that had more than 1 mm of motion in either the x, y or z direction (movement threshold). It also controlled for rotational (angular) motion, flagging time frames having more than 0.1 radians of motion around the three axes (roll, pitch and yaw) (rotation threshold). Further, ART controlled for time frames, which mean brain activation intensity differed by more than three standard deviations from the mean over all time frames of one run (z-threshold) also called 'spikes'. Spikes are artifacts caused by the scanner. The user can modify all three thresholds of this program to best fit the data of interest.

ART can only be used on data that has already been analyzed at a first-level with FSL. Following the first-level motion correction step with MCFLIRT, FSL outputs a motion parameter file that is used as an input to the ART tool. ART uses that file, as well as the functional imaging data to detect and flag outliers. Subsequently, the first-level FSL analysis has to be performed once again, this time excluding the outlying time frames of the GLM. This was performed automatically by adding an EV in the GLM for every time frame to be excluded.

Clusters in the DLPFC:

After having averaged all three runs for every subject and performed pre-threshold masking with the DLPFC, we visually inspected all subjects in 3 dimensional volumes. The goal was to assess whether an activation cluster was part of the DLPFC or not, since our definition of the DLPFC ROI is still to be improved and potentially covering too large of a territory. Also, if a subject had several clusters that could be considered as DLPFC in one hemisphere, then only the cluster with the maximally active voxel would be taken into account. We namely had to reduce the number of clusters in each hemisphere to one in order to ease this first approach in exploring the heterogeneity of the activation. An expert neuroanatomist gave final approval of the cluster selection for every subject.

5.9 Investigation of the spatial heterogeneity of the activation in the DLPFC

The following process was based on contrast 5 only, summing the activation triggered by all WM loads. Based on the COG of the clusters in the DLPFC of every individual subject, calculated by FSL, we calculated a mean COG for each hemisphere and each group, i.e. patients and controls, on which we performed a statistical test of significance to determine whether patients' mean differed from the control's. We then calculated the Euclidian distance (ED), which is a simple metric distance, of each subject's cluster's COG to the mean COG. Further, we tested whether that distance was significantly different in patients and controls.

The Euclidian distance between two points in 3 dimensions is defined as follows:

Group mean COG: mCOG = (m_x, m_y, m_z)
Individual subject's COG: iCOG = (i_x, i_y, i_z)

$$ED = \sqrt{(m_x - i_x)^2 + (m_y - i_y)^2 + (m_z - i_z)^2}$$

We calculated each population's covariance for both hemispheres and tested whether there was a significant difference between patients and controls. The covariance has the advantage of considering the 3 dimensional spatial locations of the data, which is lost in the simple measure of the ED, allowing a more meaningful analysis of the spatial heterogeneity.

6 Results

6.1 Results of the quality assurance

Disenrolled subjects:

One control got disenrolled from the study.

Behavioral criteria:

Two subjects missed four or more of the 18 SIRP blocks comprising the task. These behavioral dropouts were one patient and one control.

Missing behavioral data:

Two patients and one control had missing behavioral data for a complete run not due to subject error. They were kept for the fMRI analysis.

Freesurfer processing of the structural data:

One control and one patient were identified as having a pial surface encompassing non-brain voxels on the edge of the occipital cortex. After some minor manual edits of the structural MRI volume, the Freesurfer processing yielded a corrected pial surface.

Registration to high-resolution anatomical image:

We manually checked the registration of the functional data to the anatomical data of a subset of patients and controls. The approval of the registration for those subjects was further extrapolated onto the whole cohort.

Brainmask:

One patient had to be discarded from the analysis due to a faulty acquisition with incomplete brain coverage, hence a corrupted mask not covering the whole brain.

Motion and mean intensity:

There are 177 time frames in total in every run. One patient had over 40 outlying frames in every run (47 for run 1, 45 for run 2, and 42 for run 3) and was consequently discarded from further analysis. One control and one patient had over 50 outlying time frames in a single run (54 and 56 respectively, both in run 1). When averaging across runs, two runs showed to not give reliable results concerning the analysis of clusters of activation in the DLPFC. We therefore decided to drop those subjects from the analysis.

Two subjects had 24 (13.5%) outliers in run 1. All other runs had less than 16 (9%) outliers. All subjects with runs having less than 26 outlying time frames were retained for further analysis.

After complete QA, the average number of outlying time frames over all three runs (a total of 177x3=531 time frames) was 9 for controls and 7.5 for patients, for an average of 3 (1.7%) time frames per run for controls and 2.5 (1.4%) for patients.

Clusters in the DLPFC:

Eight subjects turned out to not have any clusters of activation in the DLPFC. Of those, five were controls and three were patients. Additionally, two controls had one cluster each in the right hemisphere, but those clusters were considered to be located too frontally. Consequently, ten subjects were not included in the calculation of the heterogeneity of the activation in the DLPFC due to lack of activation in the DLPFC.

Six subjects had more than one cluster to take into account. One control and two patients had two clusters in the left hemisphere. Two patients had two clusters in their right hemisphere. One control had two clusters in both hemispheres. In those cases, the cluster with the highest z-value at its maximally active voxel was kept for further analysis.

Out of the 47 subjects (15 controls and 32 patients), 42 (14 (93%) controls, 28 (87.5%) patients) had a cluster in the left hemisphere, and 35 (12 (80%) controls, 23 (72%) patients) had a cluster in the right hemisphere. 30 subjects had a cluster in both hemispheres (11 (73%) controls, and 19 (59%) patients). A subject not having a cluster in one of the hemisphere necessarily had one in the other. It would otherwise not have been kept for the analysis.

6.2 Group mean and group comparison

We averaged all cross-run analysis of the controls and the patients separately in order explore the general trends of activation in patients versus controls. The group analysis statistical maps for COPE 5 (summing activation caused by all three load levels) are presented on both hemispheres of one subject's inflated brain in Fig. 11 for controls and in Fig. 12 for patients. The outlines of four ROIs suggested to subserve WM are overlaid on the brain surface for easy localization of activation blobs. Those are: the DLPFC, the primary motor cortex of the hand, the intraparietal sulcus and the insula.

In addition to averaging across all subjects of one group, we performed a group comparison to test whether patients activate certain areas significantly more than controls in response to the paradigm. The group comparison statistical map is pictured in Fig. 13 overlaid on one subject's inflated brain.

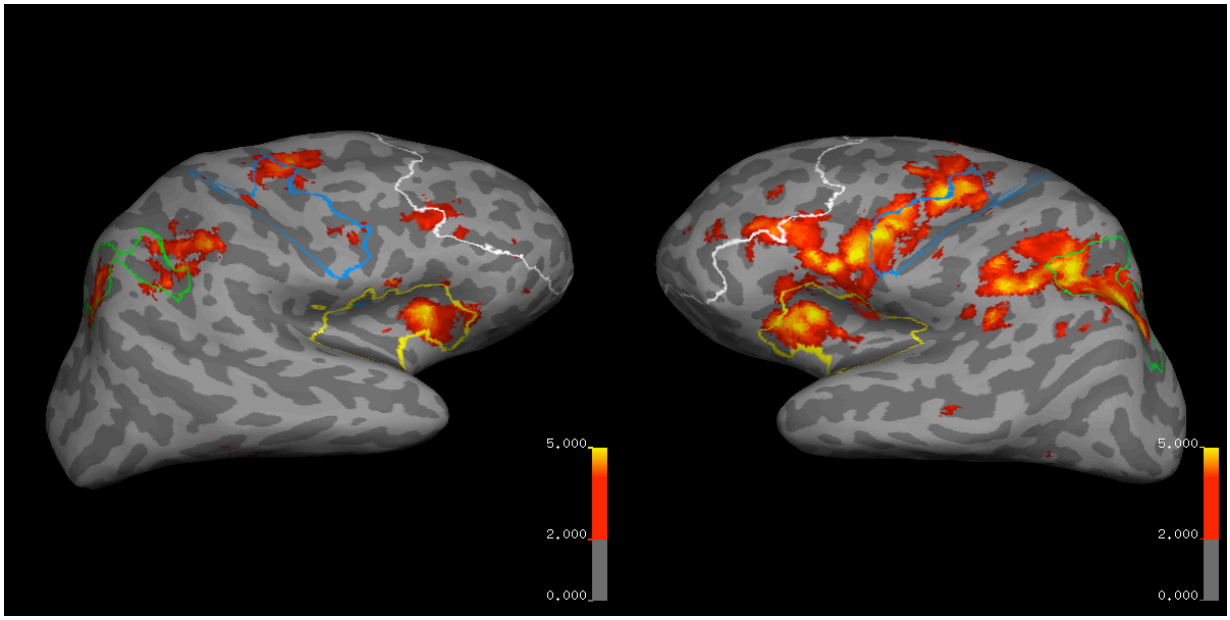

Fig. 11: Statistical map of group analysis of healthy controls overlaid on one subject's inflated brain. The map is truncated to display only positive activation. Colored outlines define ROIs: white: DLPFC; blue: primary motor cortex of the hand; green: intraparietal sulcus; yellow: insula. Color scale bar defines z level of activation. Right hemisphere is on the left.

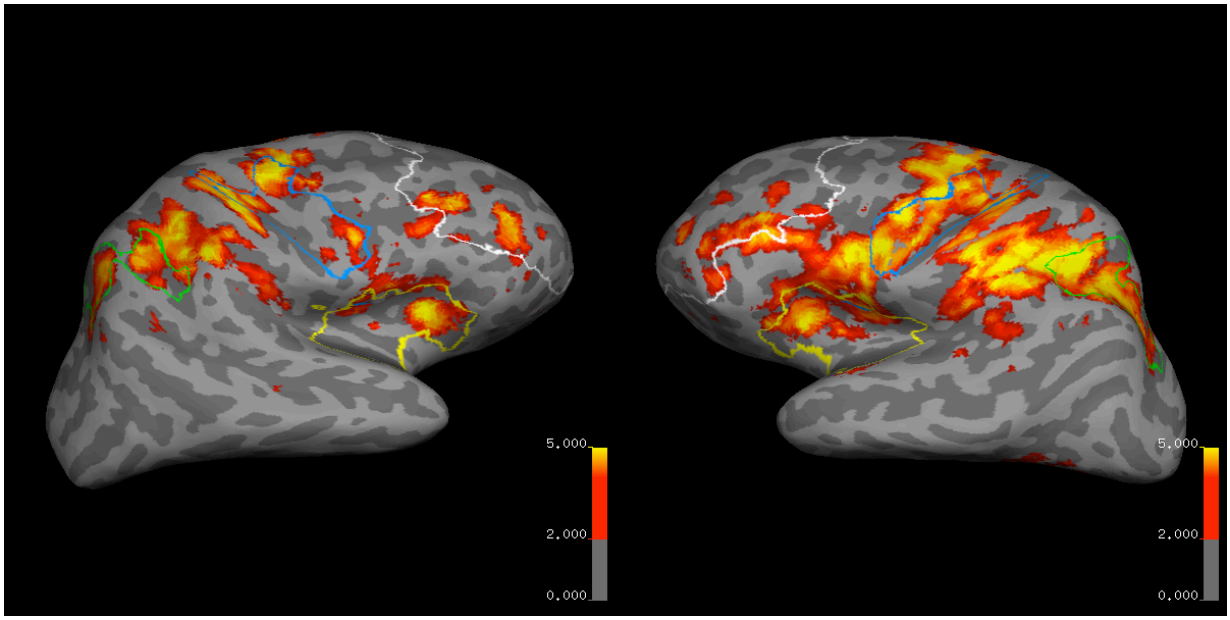

Fig. 12: Statistical map of group analysis of schizophrenia patients overlaid on one subject's inflated brain. The map is truncated to display only positive activation. Colored outlines define ROIs: white: DLPFC; blue: primary motor cortex of the hand; green: intraparietal sulcus; yellow: insula. Color scale bar defines z level of activation. Right hemisphere is on the left.

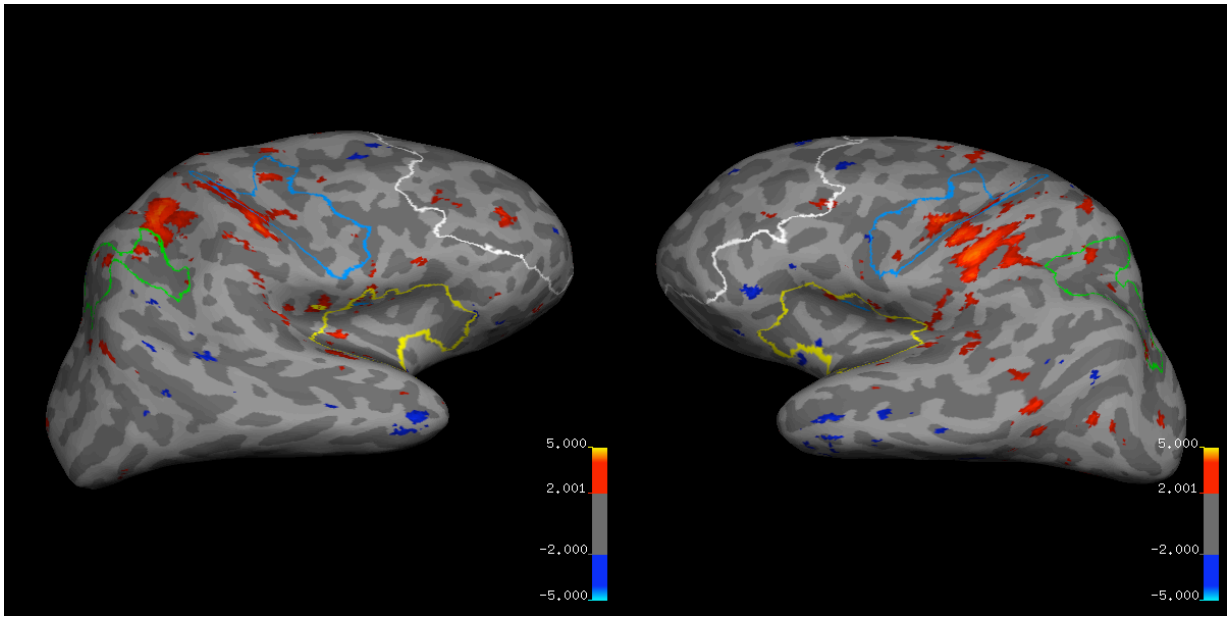

Fig. 13: Group comparison between schizophrenia patients and healthy controls overlaid on one subject's inflated brain. Warm colors show where patients activate more than controls and cold colors show where controls activate more than patients. Colored outlines define ROIs: white: DLPFC; blue: primary motor cortex of the hand; green: intraparietal sulcus; yellow: insula. Color scale bar defines z level of activation. Right hemisphere is on the left.

6.3 Study of the fMRI activation indices in the DLPFC

We started by calculating the mean of the volumes of the clusters we selected in the DLPFC. The mean volume is reported in number of voxels. We tested whether the mean cluster volume was significantly different between patients and controls in both hemispheres. There was no significant difference between patients and controls in either hemisphere with p=.33>.05 and p=.47>.05 in the left and right hemispheres respectively (see Table 4).

Table 4: Mean cluster volume in number of voxels for each group and both hemispheres, and t-tests of significance between the two groups.

	Hemisphere	**Normal subject**	**Schizophrenic subject**	**t**	**p**
Mean cluster volume (# of voxels)	left	309.27	310.97	0.99	.33
	right	344.92	305.71	0.75	.47

We computed a mean COG by averaging the spatial coordinates of each individual's cluster's COG, extracted from the FSL analysis, giving us one mean spatial coordinate vector per group and per hemisphere. The coordinates are displayed in (Table 5). To test for a significant difference between the means of the two groups we used Hotelling's T-square statistical test that is a generalization of Student's t-test for

multivariate data. The null hypothesis claims that the mean COG vectors of patients and controls are equal in a hemisphere. With a p=.66>.05 and p=.69>.05 in left and right hemispheres respectively, the null hypothesis cannot be rejected. Consequently, the mean COGs do not significantly differ between patients and controls.

Table 5: Coordinates in mm of average COG for each group and both hemisphere, and Hotelling's T-square test of significance between the means of the two groups.

	Hemisphere	Group	x	y	z	F	p
Coordinates of average COG (mm) in standard space	left	control	-36.71	42.35	19.42	0.53	.66
		schizophrenic	-37.36	43.60	17.06		
	right	control	35.53	43.04	19.30	0.49	.69
		schizophrenic	36.47	43.87	16.59		

The spatial coordinates of the average COG for each groups as well as the COG for every subject are plotted in a 3 dimensional reference frame in Fig. 14 for the left hemisphere and in Fig. 15 for the right hemisphere.

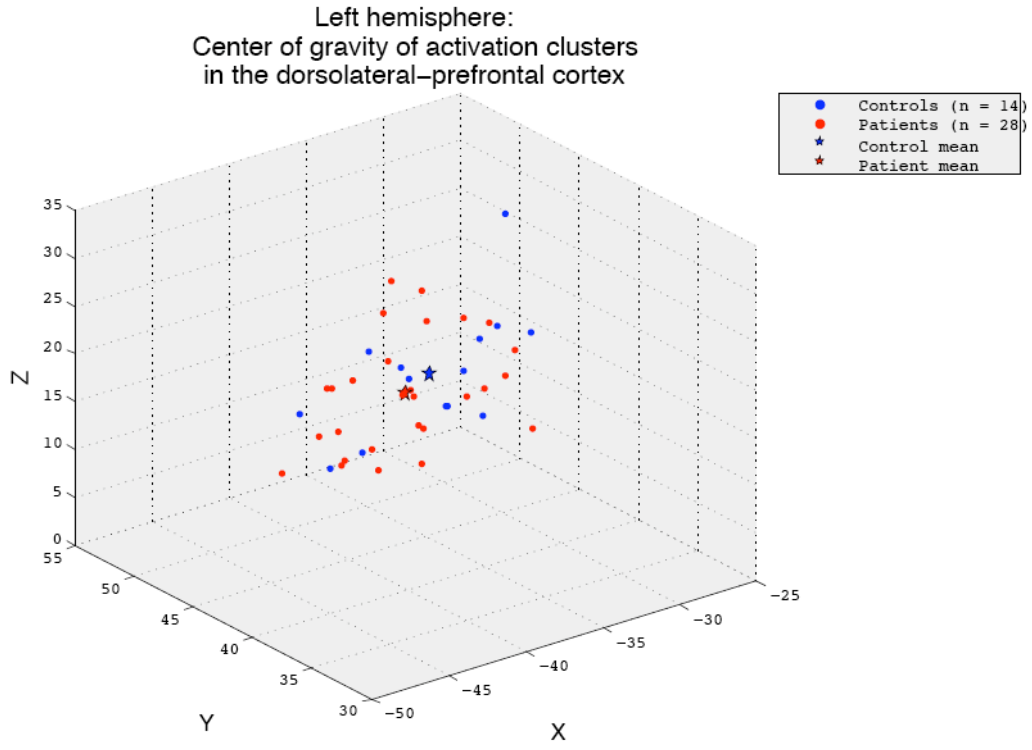

Fig. 14: Average COG and individual COG for patients and controls in the left hemisphere.

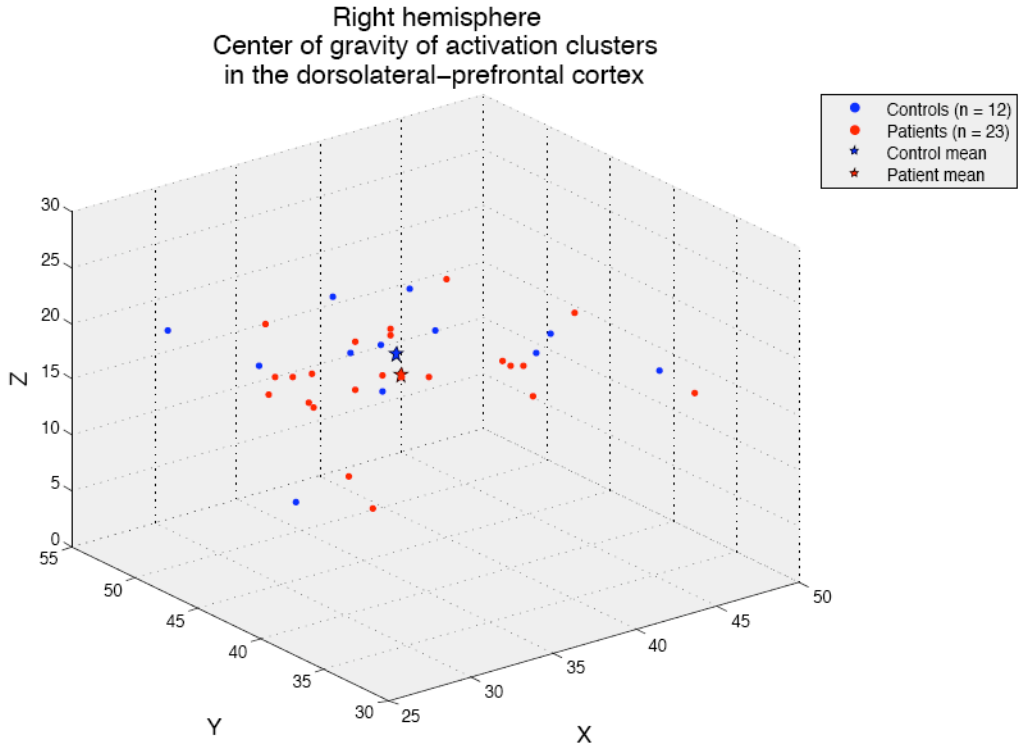

Fig. 15: Average COG and individual COG of patients and controls in the right hemisphere.

Next, we calculated the Euclidian distance (ED) from the average COG of both groups to each subject's COG. The mean of the Euclidian distances computed for both groups in each hemisphere are reported in Table 6. The EDs were tested for significance between the two groups. The distances did not show a statistically significant difference between patients and controls, as the null hypothesis of the distances being equal for patients and controls could not be rejected ($p=.78>.05$ in the left hemisphere, and $p=.38>.05$ in the right hemisphere).

Table 6: Mean and standard deviations of the Euclidian distances (mm) to the average COG of each group, and tests of significance between the two groups.

	Hemisphere	Normal subjects	Schizophrenic subjects	t	p
Mean ED distance to group COG (mm)	Left (n=42)	7.18 ± 3.63	8.55 ± 3.73	0.28	.78
	Right (n=35)	8.21 ± 3.92	8.41 ± 4.17	0.89	.38

The measure of the ED is a scalar and hence does not take into account the 3 dimensional spatial location of each COG. To consider this information, we computed

the covariance matrices of the COGs of both groups. The covariance is a measure of the extent to which the x, y, and z coordinates of the COGs vary together for each group. We tested the null hypothesis of the covariance matrices defining the COGs of patients and controls being equal using the χ^2 large-sample approximation of Box's *M* test (Box, 1949, 1950). The results are listed in Table 7. The null hypothesis could not be rejected in the right hemisphere (p-value 0.89>0.05). However, in the left hemisphere, a p-value of 0.03<0.05 rejects the null hypothesis suggesting the covariance of patients to be significantly different from controls. This means that the x, y and z coordinates of the control's COGs do not vary in the same way as the patient's ones do.

Table 7: p-value of the χ^2 large-sample approximation of Box's *M* test, testing the H_0: Cov(COGcontrols)=Cov(COGpatients) in the left and right hemispheres.

	Hemisphere	**p**
Testing equality of covariance matrices	**left**	0.03
	right	0.89

This result can be 3 dimensionally represented. The covariance matrices namely have the property of defining an ellipsoid, the eigenvectors representing the principal directions, and the inverse of the square root of the eigenvalues defining the half intensity, or equatorial radii, of its three axes. Those ellipsoids are pictured in Fig. 16 (See

Appendix A for details on the covariance matrices). The ellipsoids of both groups are plotted in the same reference frame for each hemisphere for easy visual comparison. The significant difference in the covariance of the COGs of patients and controls in the left hemisphere is suggested by that graph, as the two ellipsoids have a smaller common space coverage in the left than in the right hemisphere.

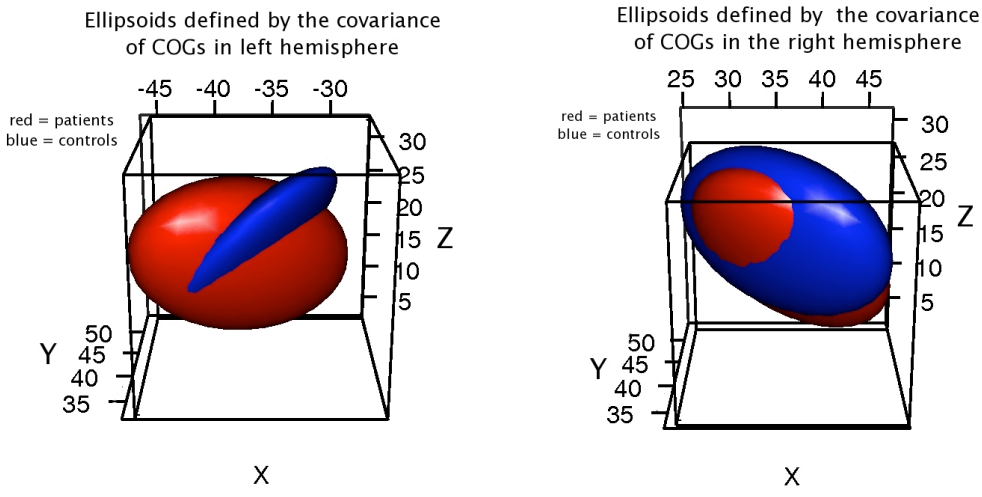

Fig. 16: Ellipsoids as defined by the covariance matrices of the COGs for patients (red) and controls (blue). Left: left hemisphere. Right: right hemisphere.

7 Discussion

Overall, schizophrenia patients and healthy controls showed activity in areas involved in the network underlying WM when performing the task in both the right and the left hemispheres, the latter showing a slightly more robust activation. The modified SIRP indeed requires some verbal processing known to be lateralized to the left hemisphere. Statistical activation maps of group averages displayed activation in the intraparietal sulcus, the insula, the primary motor regions as well as the DLPFC as seen in Fig. 11 for controls and Fig. 12 for patients. Nevertheless, patients activated all those particular regions slightly more than controls as can be seen in the group comparison map in Fig. 13, in which the red colored blobs describe where patients show more activation than controls. In fact, several controls turned out to not show any significant activation in the DLPFC, which probably contributes to the lower activation of that area in the group average of controls. This is in line with the inefficiency theory presented in Callicott et al.'s study (2003), which suggests that patients have to make more efforts in order to reach the same performance level as controls.

Our analysis was limited to the contrast showing activation of any of the three WM memory loads used in the SIRP. In order to assess for the effect of the task's load and match the patients and the controls for performance and not only for WM load (e.g. compare controls and load 5 with patients at load 1), other contrasts should be used for further analysis, such as the one comparing load 5 to load 1.

Controls showed very little activation of the DLPFC, and it was mostly localized on the posterior/inferior edge of our DLPFC ROI. Whereas patients in general recruited a more extended area of the DLPFC as we have defined it. It is to note though, that the group means and the group comparison maps are overlaid on one subject's inflated brain. That requires registration of the image from a standard stereotaxic space to the subject's native space. The ROIs as presented in Fig. 11 to Fig. 13 are therefore not representative of the whole cohort. Nevertheless, the fact that most of the activation induced by the SIRP lies on the edge of our ROI and overflows onto the VLPFC, situated inferior to the DLPFC, suggests that our search territory might benefit from an extension onto the VLPFC by including additional Freesurfer parcellations in the ROI, such as the pars triangularis and the pars opercularis together defining Broca's area in the left hemisphere. Wolf et al. (2006) have indeed found that a particular SIRP recruits the VLPFC in addition to the DLPFC.

A possible explanation for the low level of activity on the DLPFC of controls is that the task is too easy, and becomes quickly automated. The accuracy rate for this paradigm is high both for controls and patients. Following this, the SIRP used in this study might have to be improved and rendered more difficult in order to distinguish a more significant difference between the activation patterns of patients and the controls. Adding a follow up visit to the protocol may show significantly different patterns of activation between controls and patients, the latter having shown incapacity to automate the task despite steady training leading to unreliable activation patterns during two

performances of the same task separated by some amount of time. It is very likely that schizophrenia patients show less capacity in developing a strategy for handling the task causing worse performance than controls and differential recruitment of the DLPFC (Manoach, et al., 2000).

Our quality assurance process yielded artifact-free data for the group fMRI analysis, but also showed us that the data was of good quality from the beginning since we only had to drop 4 (6.25%) subjects out of the 64 because of one of our quality criteria, not considering the subject that got disenrolled from the study.

For the analysis of the COG of the clusters in the DLPFC, more subjects (mostly controls) were dropped (12 (18.75%) in addition to the 5 previously dropped). But that was solely due to the algorithm that could not take into account subjects with no data, i.e. the subjects with no clusters of activation in the DLPFC, and not due to unsatisfying data quality. Thus, controls showed less activation than patients in the DLPFC, but by comparing only the subjects of both groups that did have clusters in the DLPFC, the volume (in number of voxels) of those clusters did not differ.

The Euclidian distance between each subject's cluster's COG to the group's mean COG in both the right and the left hemisphere was not significantly different between schizophrenia patients and healthy controls. The mean COG of the clusters of activity did not differ between both groups. The covariance of the COGs of patients and controls was significantly different in the left hemisphere, but not in the right. The statistical test does not tell us what group has a bigger variance than the other. Nevertheless, the determinant of the covariance matrix is correlated to the extent of the covariance. In this case, the covariance matrix of the patients had a determinant of one order of magnitude bigger than the controls in the left hemisphere (see Appendix A). In the left hemisphere, the mean of the COGs does not significantly differ, while the covariance does, which indicates a greater scatter of the COGs in patients relative to controls. This suggests that schizophrenia patients show significantly greater spatial heterogeneity of the indices of activation evoked by the WM paradigm in the DLPFC of the left hemisphere as proposed by Manoach et al. (2000). A greater spatial heterogeneity of DLPFC activation in schizophrenia patients could potentially be correlated to white matter abnormalities. The same conclusion cannot be drawn for the right hemisphere.

The methods we used for the analysis of the spatial localization of fMRI activation indices in the DLPFC were a first approach to that particular aspect of this study. We will now discuss their limitations.

fMRI data is inherently noisy. The amplitude of the BOLD signal that is of interest for the analysis of the functionality of the brain is not much larger than the noise and hence difficult to extract from it.

FSL is a MRI analysis tool in constant development and the way in which it computes the COG of an activation cluster might not be the most representative of the data. Moreover, the clusters for which the COG was calculated were limited to the white/gray matter border, because we filtered the data with ROIs that are surface based

(i.e. surface-based labels following the white/gray matter intersection), which somewhat biases the data on which the COG is computed. Even though the surface of the brain is where we expect the actual BOLD activation, and knowing the fact that the smoothing performed during the preprocessing of the data contributes to spreading the signal beyond the surface into the white matter. The computation of the COG might be more realistic with the use of an ROI, which thickness is dilated of a couple of voxels in order to cover a more consistent area of the activation. By filtering the data with such a limited area and performing cluster based correction for false positives our analysis may have become too conservative and rejected true positives.

Further, we had to visually inspect all subjects in order to select the clusters of interest in the DLPFC, because some subjects had activation in the very frontal and superior parts of the ROI that should not be included in the DLPFC according to our study of the literature on DLPFC delimitation. Following this, to ease the analysis, the ROI could be reduced in size by applying a frontal cut at the Talairach coordinate y=53 based of the cytoarchitectonic study performed by Rajkowska & Goldman-Rakic (1995b). On the other hand, by excluding clusters located too frontally and too superiorly, we may have been too conservative in assuming the spatial location of the DLPFC, and discarded brain areas actually subserving WM. Most cytoarchitectonic studies defining the DLPFC are based on normal controls and not patients with brain disorders. Neuropsychiatric disorders such as schizophrenia may lead to modification in the cytoarchitechtonics and/or anatomy. In such a case, the DLPFC needs to be specifically defined for patients, which was not the case in this study. Park et al. (2004) have pointed out how the definition of several ROIs differ in schizophrenia patients with the use of probability maps.

In particular, the location of the DLPFC is quite variable across subjects (Rajkowska & Goldman-Rakic, 1995b). Potentially, this variability is even greater among schizophrenic subjects (Manoach, 2003). Brain imaging analysis attempts to correct for that variation across subjects by performing spatial normalization and smoothing of the data. However, most spatial normalization algorithms are based on the anatomy of healthy subjects. An asset of our definition of the DLPFC is that it is specific for each subject based on its Freesurfer cortical parcellation.

In parallel to using the DLPFC for the analysis, we could use a control ROI covering an area known to be involved in the processing of WM tasks but that has not been suggested to show any particular spatial heterogeneity of activation in schizophrenia patients, such as the intraparietal sulcus.

All calculations related to the COG were based on only one cluster per subject and per hemisphere. In some cases, several clusters were eligible to be included in the DLPFC but only one could be included for the algorithm to work. This might have biased the results by reducing heterogeneity of activation to only one location. Another bias is that many controls were dropped due to having no clusters in the DLPFC. We would like to find a method allowing for several clusters to be taken into account in one hemisphere and also find a way of taking into account the subjects that do not show any activation.

Other factors that can have an effect of the brain activation patterns in schizophrenia patients are for example, the genetic aspects of the disease (e.g. effect of COMT and MTHFR), the antipsychotic treatment, or the smoking history of the patients. In this study those features certainly contributed to the variability of the data but are not corrected for.

8 Conclusion

On average, both schizophrenia patients and controls showed activation in the brain regions expected to be recruited for the use of WM. The activation tended to be more robust in the left hemisphere. The hypothesis suggesting that patients show more spatially scattered activation in the DLPFC than controls while performing a task requiring the use of WM was supported by our findings in the left hemisphere, but not in the right one. Indeed, patients did show significantly greater covariance, relative to healthy controls, of the localizations of the COGs of activation clusters in the DLPFC of the left hemisphere in response to a task requiring WM. Even though the spatial scatter of the COGs was more heterogeneous for patients, the Euclidian distance to the group's mean COG did not significantly differ between controls and patients.

We performed a careful quality assurance before processing the data. Nevertheless, it is of note that the methods developed for this particular study have limitations that would be worth correcting for in order to replicate our results and confirm the hypothesis. Those limitations are considered in the discussion, and lead to future ideas for the investigation of the matter.

9 References

American Psychiatric Association (1994). *Diagnostic and Statistical Manual of Mental Disorders* (4th ed.). Washington, DC: American Psychiatric Association.

Baddeley, A. (1992). Working memory. *Science, 255*(5044), 556-559.

Barch, D. M., Carter, C. S., Braver, T. S., Sabb, F. W., MacDonald, A., 3rd, Noll, D. C., et al. (2001). Selective deficits in prefrontal cortex function in medication-naive patients with schizophrenia. *Arch Gen Psychiatry, 58*(3), 280-288.

Berman, K. F., Torrey, E. F., Daniel, D. G., & Weinberger, D. R. (1992). Regional cerebral blood flow in monozygotic twins discordant and concordant for schizophrenia. *Arch Gen Psychiatry, 49*(12), 927-934.

Berman, K. F., Zec, R. F., & Weinberger, D. R. (1986). Physiologic dysfunction of dorsolateral prefrontal cortex in schizophrenia. II. Role of neuroleptic treatment, attention, and mental effort. *Arch Gen Psychiatry, 43*(2), 126-135.

Biomedical Informatics Research Network (BIRN). 2009, from http://www.nbirn.net/

Box, G. E. P. (1949). A general distribution theory for a clall of likelihood criteria. *Biometrika, 36*, 317-346.

Box, G. E. P. (1950). Problems in the analysis of growth and linear curves. *Biometrics, 6*, 362-389.

Brodmann, K. (1909). Vergleichende Localisationslehre der Grosshirnrinde in ihren Prinzipien dargestellt auf Grund des Zellenbaue. In J. A. Barth (Ed.). Leipzig.

Callicott, J. H., Bertolino, A., Mattay, V. S., Langheim, F. J., Duyn, J., Coppola, R., et al. (2000). Physiological dysfunction of the dorsolateral prefrontal cortex in schizophrenia revisited. *Cereb Cortex, 10*(11), 1078-1092.

Callicott, J. H., Mattay, V. S., Bertolino, A., Finn, K., Coppola, R., Frank, J. A., et al. (1999). Physiological characteristics of capacity constraints in working memory as revealed by functional MRI. *Cereb Cortex, 9*(1), 20-26.

Callicott, J. H., Mattay, V. S., Verchinski, B. A., Marenco, S., Egan, M. F., & Weinberger, D. R. (2003). Complexity of prefrontal cortical dysfunction in schizophrenia: more than up or down. *Am J Psychiatry, 160*(12), 2209-2215.

Cannon, T. D., Glahn, D. C., Kim, J., Van Erp, T. G., Karlsgodt, K., Cohen, M. S., et al. (2005). Dorsolateral prefrontal cortex activity during maintenance and manipulation of information in working memory in patients with schizophrenia. *Arch Gen Psychiatry, 62*(10), 1071-1080.

Cohen, J. D., Perlstein, W. M., Braver, T. S., Nystrom, L. E., Noll, D. C., Jonides, J., et al. (1997). Temporal dynamics of brain activation during a working memory task. *Nature, 386*(6625), 604-608.

Daniel, D. G., Zigun, J. R., & Weinberger, D. R. (1994). Brain imaging and neuropsychiatry. In S. C. Yudofsky & R. E. Hales (Eds.), *Synopsis of Neuropsychiatry* (pp. 143-156). Washington, DC: American Psychiatric Press, Inc.

Driesen, N. R., Leung, H. C., Calhoun, V. D., Constable, R. T., Gueorguieva, R., Hoffman, R., et al. (2008). Impairment of working memory maintenance and response in schizophrenia: functional magnetic resonance imaging evidence. *Biol Psychiatry, 64*(12), 1026-1034.

Dronkers, N. F., Plaisant, O., Iba-Zizen, M. T., & Cabanis, E. A. (2007). Paul Broca's historic cases: high resolution MR imaging of the brains of Leborgne and Lelong. *Brain, 130*(Pt 5), 1432-1441.

English Wiktionary. (2009).

Farde, L., Wiesel, F. A., Stone-Elander, S., Halldin, C., Nordstrom, A. L., Hall, H., et al. (1990). D2 dopamine receptors in neuroleptic-naive schizophrenic patients. A positron emission tomography study with [11C]raclopride. *Arch Gen Psychiatry, 47*(3), 213-219.

FIPS Wiki. 2009, from https://xwiki.nbirn.net/xwiki/bin/view/Project-FIPS-Public/Home

Fischl, B., Salat, D. H., Busa, E., Albert, M., Dieterich, M., Haselgrove, C., et al. (2002). Whole brain segmentation: automated labeling of neuroanatomical structures in the human brain. *Neuron, 33*(3), 341-355.

Forman, S. D., Cohen, J. D., Fitzgerald, M., Eddy, W. F., Mintun, M. A., & Noll, D. C. (1995). Improved assessment of significant activation in functional magnetic resonance imaging (fMRI): use of a cluster-size threshold. *Magn Reson Med, 33*(5), 636-647.

Freesurfer surface reconstruction software. 2009, from http://surfer.nmr.mgh.harvard.edu/

Friston, K. J., Worsley, K. J., Frakowiak, R. S. J., Mazziotta, J. C., & Evans, A. C. (1994). Assessing the significance of focal activations using their spatial extent. *Hum Brain Map, 1*, (214-220).

FSL - FMRIB Software Library. 2009, from http://www.fmrib.ox.ac.uk/fsl

Goldberg, T. E., Berman, K. F., Fleming, K., Ostrem, J., Van Horn, J. D., Esposito, G., et al. (1998). Uncoupling cognitive workload and prefrontal cortical physiology: a PET rCBF study. *Neuroimage, 7*(4 Pt 1), 296-303.

Goldberg, T. E., & Weinberger, D. R. (1996). Effects of neuroleptic medications on the cognition of patients with schizophrenia: a review of recent studies. *J Clin Psychiatry, 57 Suppl 9*, 62-65.

Goldman-Rakic, P. S. (1994). Working memory dysfunction in schizophrenia. *J Neuropsychiatry Clin Neurosci, 6*(4), 348-357.

Green, M. F. (1996). What are the functional consequences of neurocognitive deficits in schizophrenia? *Am J Psychiatry, 153*(3), 321-330.

Green, M. F., Marshall, B. D., Jr., Wirshing, W. C., Ames, D., Marder, S. R., McGurk, S., et al. (1997). Does risperidone improve verbal working memory in treatment-resistant schizophrenia? *Am J Psychiatry, 154*(6), 799-804.

Gur, R. E., Calkins, M. E., Gur, R. C., Horan, W. P., Nuechterlein, K. H., Seidman, L. J., et al. (2007). The Consortium on the Genetics of Schizophrenia: neurocognitive endophenotypes. *Schizophr Bull, 33*(1), 49-68.

Holt, J. L., Van Horn, J. D., Meyer-Lindenberg, A., & al. (1999). *Multiple sources of signal abnormality underlying prefrontal hypofunction and increased variability in the sites of activation within BA 9/46 in individual medication free schizophrenic patients*. Paper presented at the Siciety for Neuroscience.

Huettel, S. A., Song, A. W., & McCarthy, G. (2004). *Functional Magnetic Resonance Imaging*. Sunderland, MA: Sinauer Associates, Inc.

Ingvar, D. H., & Franzen, G. (1974). Distribution of cerebral activity in chronic schizophrenia. *Lancet, 2*(7895), 1484-1486.

Jenkinson, M., Bannister, P., Brady, M., & Smith, S. (2002). Improved optimization for the robust and accurate linear registration and motion correction of brain images. *Neuroimage, 17*(2), 825-841.

Jenkinson, M., & Smith, S. (2001). A global optimisation method for robust affine registration of brain images. *Med Image Anal, 5*(2), 143-156.

Jonides, J., Schumacher, E. H., Smith, E. E., Koeppe, R. A., Awh, E., Reuter-Lorenz, P. A., et al. (1998). The role of parietal cortex in verbal working memory. *J Neurosci, 18*(13), 5026-5034.

Kandel, E. R., Schwartz, J. H., & Jessell, T. M. (Eds.). (2000). *Principles of Neural Science* (4th ed.). U.S.A.: McGraw-Hill Companies, Inc.

Karlsgodt, K. H., Sanz, J., van Erp, T. G., Bearden, C. E., Nuechterlein, K. H., & Cannon, T. D. (2009). Re-evaluating dorsolateral prefrontal cortex activation during working memory in schizophrenia. *Schizophr Res, 108*(1-3), 143-150.

Karlsgodt, K. H., van Erp, T. G., Poldrack, R. A., Bearden, C. E., Nuechterlein, K. H., & Cannon, T. D. (2008). Diffusion tensor imaging of the superior longitudinal fasciculus and working memory in recent-onset schizophrenia. *Biol Psychiatry, 63*(5), 512-518.

Makris, N., Kennedy, D. N., McInerney, S., Sorensen, A. G., Wang, R., Caviness, V. S., Jr., et al. (2005). Segmentation of subcomponents within the superior longitudinal fascicle in humans: a quantitative, in vivo, DT-MRI study. *Cereb Cortex, 15*(6), 854-869.

Maldjian, J. A., Laurienti, P. J., & Burdette, J. H. (2004). Precentral gyrus discrepancy in electronic versions of the Talairach atlas. *Neuroimage, 21*(1), 450-455.

Maldjian, J. A., Laurienti, P. J., Kraft, R. A., & Burdette, J. H. (2003). An automated method for neuroanatomic and cytoarchitectonic atlas-based interrogation of fMRI data sets. *Neuroimage, 19*(3), 1233-1239.

Manoach, D. S. (2003). Prefrontal cortex dysfunction during working memory performance in schizophrenia: reconciling discrepant findings. *Schizophr Res, 60*(2-3), 285-298.

Manoach, D. S., Gollub, R. L., Benson, E. S., Searl, M. M., Goff, D. C., Halpern, E., et al. (2000). Schizophrenic subjects show aberrant fMRI activation of dorsolateral prefrontal cortex and basal ganglia during working memory performance. *Biol Psychiatry, 48*(2), 99-109.

Manoach, D. S., Press, D. Z., Thangaraj, V., Searl, M. M., Goff, D. C., Halpern, E., et al. (1999). Schizophrenic subjects activate dorsolateral prefrontal cortex during a working memory task, as measured by fMRI. *Biol Psychiatry, 45*(9), 1128-1137.

Manoach, D. S., Schlaug, G., Siewert, B., Darby, D. G., Bly, B. M., Benfield, A., et al. (1997). Prefrontal cortex fMRI signal changes are correlated with working memory load. *Neuroreport, 8*(2), 545-549.

Martinot, J. L., Peron-Magnan, P., Huret, J. D., Mazoyer, B., Baron, J. C., Boulenger, J. P., et al. (1990). Striatal D2 dopaminergic receptors assessed with positron emission tomography and [76Br]bromospiperone in untreated schizophrenic patients. *Am J Psychiatry, 147*(1), 44-50.

McCarthy, G., Puce, A., Constable, R. T., Krystal, J. H., Gore, J. C., & Goldman-Rakic, P. (1996). Activation of human prefrontal cortex during spatial and nonspatial working memory tasks measured by functional MRI. *Cereb Cortex, 6*(4), 600-611.

Montreal Neurological Institute. Retrieved 2009, from www.mni.mcgill.ca

NIMH: What are the symptoms of schizophrenia (2009). Retrieved June 7, 2009, from http://www.nimh.nih.gov/health/publications/schizophrenia/what-are-the-symptoms-of-schizophrenia.shtml

Owen, A. M. (2000). The role of the lateral frontal cortex in mnemonic processing: the contribution of functional neuroimaging. *Exp Brain Res, 133*(1), 33-43.

Owen, A. M., Sahakian, B. J., Semple, J., Polkey, C. E., & Robbins, T. W. (1995). Visuo-spatial short-term recognition memory and learning after temporal lobe excisions, frontal lobe excisions or amygdalo-hippocampectomy in man. *Neuropsychologia, 33*(1), 1-24.

Oxford American Dictionaries. (2005). Application for Macintosh, version 1.0.2.

Pandya, D. N., & Barnes, C. L. (1987). Architecture and connections of the frontal lobe. In E. Perecman (Ed.), *The Frontal Lobes Revisited* (pp. 41-72). New York: IRBN Press.

Park, H. J., Levitt, J., Shenton, M. E., Salisbury, D. F., Kubicki, M., Kikinis, R., et al. (2004). An MRI study of spatial probability brain map differences between first-episode schizophrenia and normal controls. *Neuroimage, 22*(3), 1231-1246.

Park, S., & Holzman, P. S. (1992). Schizophrenics show spatial working memory deficits. *Arch Gen Psychiatry, 49*(12), 975-982.

Petrides, M. (1996). Specialized systems for the processing of mnemonic information within the primate frontal cortex. *Philos Trans R Soc Lond B Biol Sci, 351*(1346), 1455-1461; discussion 1461-1452.

Petrides, M., Alivisatos, B., Meyer, E., & Evans, A. C. (1993). Functional activation of the human frontal cortex during the performance of verbal working memory tasks. *Proc Natl Acad Sci U S A, 90*(3), 878-882.

Petrides, M., & Milner, B. (1982). Deficits on subject-ordered tasks after frontal- and temporal-lobe lesions in man. *Neuropsychologia, 20*(3), 249-262.

Petrides, M., & Pandya, D. N. (1984). Projections to the frontal cortex from the posterior parietal region in the rhesus monkey. *J Comp Neurol, 228*(1), 105-116.

Petrides, M., & Pandya, D. N. (1999). Dorsolateral prefrontal cortex: comparative cytoarchitectonic analysis in the human and the macaque brain and corticocortical connection patterns. *Eur J Neurosci, 11*(3), 1011-1036.

Potkin, S. G., Turner, J. A., Guffanti, G., Lakatos, A., Fallon, J. H., Nguyen, D. D., et al. (2009). A genome-wide association study of schizophrenia using brain activation as a quantitative phenotype. *Schizophr Bull, 35*(1), 96-108.

Ragland, J. D., Yoon, J., Minzenberg, M. J., & Carter, C. S. (2007). Neuroimaging of cognitive disability in schizophrenia: search for a pathophysiological mechanism. *Int Rev Psychiatry, 19*(4), 417-427.

Rajkowska, G., & Goldman-Rakic, P. S. (1995a). Cytoarchitectonic definition of prefrontal areas in the normal human cortex: I. Remapping of areas 9 and 46 using quantitative criteria. *Cereb Cortex, 5*(4), 307-322.

Rajkowska, G., & Goldman-Rakic, P. S. (1995b). Cytoarchitectonic definition of prefrontal areas in the normal human cortex: II. Variability in locations of areas 9 and 46 and relationship to the Talairach Coordinate System. *Cereb Cortex, 5*(4), 323-337.

Reus, V. I. (2008). Mental Disorders: Schizophrenia. In A. Fauci, E. Braunwald, D. Kasper, S. Hauser, D. Longo, J. Jameson & J. Loscalzo (Eds.), Harrison's Principles of Internal Medicine, 17th Edition Available from http://phstwlp1.partners.org:2270/content.aspx?aID=2908190

Roffman, J. L., Gollub, R. L., Calhoun, V. D., Wassink, T. H., Weiss, A. P., Ho, B. C., et al. (2008). MTHFR 677C --> T genotype disrupts prefrontal function in schizophrenia through an interaction with COMT 158Val --> Met. *Proc Natl Acad Sci U S A, 105*(45), 17573-17578.

Roffman, J. L., Weiss, A. P., Deckersbach, T., Freudenreich, O., Henderson, D. C., Wong, D. H., et al. (2008). Interactive effects of COMT Val108/158Met and MTHFR C677T on executive function in schizophrenia. *Am J Med Genet B Neuropsychiatr Genet, 147B*(6), 990-995.

Rypma, B., Prabhakaran, V., Desmond, J. E., Glover, G. H., & Gabrieli, J. D. (1999). Load-dependent roles of frontal brain regions in the maintenance of working memory. *Neuroimage, 9*(2), 216-226.

Sarkissov, S. A., Filimonoff, I. N., Konokova, I. P., Preobrazenskaja, N. S., & Kukueva, L. A. (Eds.). (1955). *Atlas of the cytoarchitectonics of the human cerebral cortex [in Russian]*. Moscow: Medgiz.

Sawaguchi, T., & Goldman-Rakic, P. S. (1991). D1 dopamine receptors in prefrontal cortex: involvement in working memory. *Science, 251*(4996), 947-950.

Schlosser, R., Gesierich, T., Kaufmann, B., Vucurevic, G., Hunsche, S., Gawehn, J., et al. (2003). Altered effective connectivity during working memory performance in schizophrenia: a study with fMRI and structural equation modeling. *Neuroimage, 19*(3), 751-763.

Schlosser, R., Hutchinson, M., Joseffer, S., Rusinek, H., Saarimaki, A., Stevenson, J., et al. (1998). Functional magnetic resonance imaging of human brain activity in a verbal fluency task. *J Neurol Neurosurg Psychiatry, 64*(4), 492-498.

Schlosser, R. G., Nenadic, I., Wagner, G., Gullmar, D., von Consbruch, K., Kohler, S., et al. (2007). White matter abnormalities and brain activation in schizophrenia: a combined DTI and fMRI study. *Schizophr Res, 89*(1-3), 1-11.

Selemon, L. D., Mrzljak, J., Kleinman, J. E., Herman, M. M., & Goldman-Rakic, P. S. (2003). Regional specificity in the neuropathologic substrates of schizophrenia: a morphometric analysis of Broca's area 44 and area 9. *Arch Gen Psychiatry, 60*(1), 69-77.

Smith, E. E., Jonides, J., Marshuetz, C., & Koeppe, R. A. (1998). Components of verbal working memory: evidence from neuroimaging. *Proc Natl Acad Sci U S A, 95*(3), 876-882.

Smith, S. M. (2002). Fast robust automated brain extraction. *Hum Brain Mapp, 17*(3), 143-155.

Sternberg, S. (1966). High-speed scanning in human memory. *Science, 153*(736), 652-654.

Stevens, A. A., Goldman-Rakic, P. S., Gore, J. C., Fulbright, R. K., & Wexler, B. E. (1998). Cortical dysfunction in schizophrenia during auditory word and tone working memory demonstrated by functional magnetic resonance imaging. *Arch Gen Psychiatry, 55*(12), 1097-1103.

Strub, R. L., & Wise, M. G. (1994). Differential diagnosis in neuropsychiatry. In S. C. Yudofsky & R. E. Hales (Eds.), *Synopsis in Neuropsychiatry*. Washington, DC: American Psychiatric Press, Inc.

Sullivan, E. V., Mathalon, D. H., Zipursky, R. B., Kersteen-Tucker, Z., Knight, R. T., & Pfefferbaum, A. (1993). Factors of the Wisconsin Card Sorting Test as measures of frontal-lobe function in schizophrenia and in chronic alcoholism. *Psychiatry Res, 46*(2), 175-199.

Talairach, J., & Tournoux, P. (1988). *Co-planar stereotaxic atlas of the human brain*. Stuttgart: Thieme.

Tranel, D. (1994). Functional neuroanatomy from a neuropsychological perspective. In S. C. Yudofsky & R. E. Hales (Eds.), *Synopsis of Neuropsychiatry* (pp. 49-74). Washington, DC: American Psychiatric Press, Inc.

Uylings, H. B., Rajkowska, G., Sanz-Arigita, E., Amunts, K., & Zilles, K. (2005). Consequences of large interindividual variability for human brain atlases: converging macroscopical imaging and microscopical neuroanatomy. *Anat Embryol (Berl), 210*(5-6), 423-431.

von Economo, C., & Koskinas, G. N. (1925). *Die cytoarchitectonic der Hirnrinde des erwachsenen Menchen*. Berlin: Springer.

Weinberger, D. R., & Berman, K. F. (1996). Prefrontal function in schizophrenia: confounds and controversies. *Philos Trans R Soc Lond B Biol Sci, 351*(1346), 1495-1503.

Weinberger, D. R., Berman, K. F., & Zec, R. F. (1986). Physiologic dysfunction of dorsolateral prefrontal cortex in schizophrenia. I. Regional cerebral blood flow evidence. *Arch Gen Psychiatry, 43*(2), 114-124.

Whitfield-Gabrieli, S. (2009). Artifact Detection Tools, from http://web.mit.edu/swg/software.htm

Wisco, J. J., Kuperberg, G., Manoach, D., Quinn, B. T., Busa, E., Fischl, B., et al. (2007). Abnormal cortical folding patterns within Broca's area in schizophrenia: evidence from structural MRI. *Schizophr Res, 94*(1-3), 317-327.

Wolf, R. C., Vasic, N., & Walter, H. (2006). Differential activation of ventrolateral prefrontal cortex during working memory retrieval. *Neuropsychologia, 44*(12), 2558-2563.

Wong, D. F., Wagner, H. N., Jr., Tune, L. E., Dannals, R. F., Pearlson, G. D., Links, J. M., et al. (1986). Positron emission tomography reveals elevated D2 dopamine receptors in drug-naive schizophrenics. *Science, 234*(4783), 1558-1563.

Worsley, K. J., Evans, A. C., Marrett, S., & Neelin, P. (1992). A three-dimensional statistical analysis for CBF activation studies in human brain. *J Cereb Blood Flow Metab, 12*(6), 900-918.

Yudofsky, S. C., & Hales, R. E. (Eds.). (1994). *Synopsis of Neuropsychiatry* (1st ed.). Washington, DC: American Psychiatric Press, Inc.

Zigun, J. R., & Weinberger, D. R. W. (1992). In vivo studies of brain morphology in schizophrenia. In J.-P. Lindenmayerand & R. K. Stanley (Eds.), *New Biological Vistas on Schizophrenia* (pp. 57-81). New York: Brunner/Mazel.

10 Appendix A

Left hemisphere

Controls:

Covariance matrix SL1 =
11.0598 2.3369 13.1365
2.3369 22.5442 -14.3742
13.1365 -14.3742 36.0018

Determinant of SL1:
det(SL1) = 1.7218e+03

Eigenvectors (each column represents an eigenvector):
VL1 =
-0.7768 0.5674 0.2731
0.4155 0.7878 -0.4546
0.4731 0.2397 0.8478

Eigenvalues:
λ_1 = 1.8089
λ_2 = 19.8539
λ_3 = 47.9430

Patients:

Covariance matrix SL2 =
19.3846 11.4895 -5.9811
11.4895 26.8048 -20.6537
-5.9811 -20.6537 44.0426

Determinant of SL2:
det(SL2) = 1.0681e+04

Eigenvectors (each column represents an eigenvector):
VL2 =
0.5918 0.7603 -0.2680
-0.7366 0.3749 -0.5629

-0.3275 0.5305 0.7819

Eigenvalues:
λ_1 = 8.3927
λ_2 = 20.8766
λ_3 = 60.9627

Right hemisphere

Controls:

Covariance matrix SR1 =
27.4930 -15.5484 -2.6141
-15.5484 27.6845 -13.5284
-2.6141 -13.5284 35.0878

Determinant of SR1:
det(SR1) = 1.1903e+04

Eigenvectors (each column represents an eigenvector):
VR1 =
0.5885 -0.6874 0.4256
0.7050 0.1786 -0.6864
0.3958 0.7040 0.5897

Eigenvalues:
λ_1 = 7.1087
λ_2 = 34.2088
λ_3 = 48.9477

Patients:

Covariance matrix SR2 =
24.6200 -3.5124 -10.5928
-3.5124 25.9029 -21.8930
-10.5928 -21.8930 41.5878

Determinant of SR2:
det(SR2) = 9.6726e+03

Eigenvectors (each column represents an eigenvector):

VR2 =

0.4495	0.8700	-0.2026
0.6952	-0.4831	-0.5323
0.5609	-0.0984	0.8220

Eigenvalues:
$\lambda_1 = 5.9671$
$\lambda_2 = 27.7685$
$\lambda_3 = 58.3751$